Before the electrodes were removed, MRI was performed to confirm the locations of the electrodes. MRI findings confirmed that in all patients, the amygdalar depth electrodes were placed correctly, and the hippocampal depth electrodes were placed in the subiculum or Ammon's horn.

After completing the invasive monitoring, 13 patients underwent amygdalohippocampectomy, three anterior temporal lobectomy, including medial temporal structures, and one lateral temporal resection sparing the medial temporal structures. The remaining two patients did not undergo resective surgery. Postoperative follow-up ranged from 12 to 54 months.

2.2. Visual inspection of ictal HFO

The ictal EEGs were analyzed visually for the presence of distinct oscillations with frequencies of 200 Hz and higher (fast ripples) by two clinical epileptologists (N.U. and K.T.). Both observers jointly reviewed the data and established a consensus. High frequency activities slower than 200 Hz (ripples) were not analyzed in the current study. To visualize high frequency activities, the horizontal (time) and vertical (amplitude) axes of the EEG display were expanded, and the signals were digitally high-pass filtered at 50 Hz (time constant of 0.003 s). HFO were defined as follows: (1) appearing on several occasions at a similar frequency in the same channel; (2) visually detectable as sinusoidal waves, and (3) containing at least four consecutive peaks with similar inter-peak intervals. Typical examples of ictal HFO are shown in Figs. 2–4. The frequencies, amplitudes, locations, durations and intervals of HFO were measured on the CRT screen. Moreover, total durations of HFO events, as well as the intervals between HFO onset and EEG onset on conventional EEG, were also measured. Seizure onset on conventional EEG was defined as localized, sustained, rhythmic, or spiking EEG pattern with a frequency >2 Hz, visually distinguished from background activity (Spencer et al., 1992). Ictal EEG was reviewed 5 min before EEG onset defined by conventional EEG. Interictal EEG of 5 min was also reviewed in each patient. The state (awake or asleep) of the patients during interictal recording was variable. In 15 patients, the interictal data were more than 2 h away from the seizures. However, the interictal data were within 2 h (30 min away from seizures in one patient, 40 min in two, and 1 h and 40 min in one) from seizures in the remaining four patients. In patients who had interictal HFO, the onset of ictal HFO were defined as the time at which HFO appeared regularly and the interval of HFO became shorter than 3 s. In patients who had interictal HFO with a mean interval of less than 3 s, the onset of ictal HFO were defined as the time at which the mean interval of HFO became shorter than 1 s.

2.3. Correlation with hippocampal pathology and seizure outcome

In 16 patients who underwent medial temporal resection, the degree of hippocampal neuron loss in the resected specimens was evaluated. Hippocampal pathology was classified using Blűmcke's classification (Blűmcke et al., 2007) as follows: no MTS: normal hippocampus, MTS type 1a: classic hippocampal sclerosis with severe cell loss in CA1and moderate loss in remaining sectors, MTS type 1b: severe hippocampal sclerosis affecting all hippocampal sectors, MTS type 2: severe cell loss in CA1 and only mild pathology within remaining sectors (i.e. CA1-sclerosis), MTS type 3: end folium sclerosis with moderate cell loss in all sectors with exception of CA1.

Seizure outcomes were evaluated using Engel's criteria. The relations between the presence of ictal HFO, pathology of resected hippocampi, and postoperative seizure outcome were analyzed statistically by using Fisher's exact probability test. An error probability of less than 0.05 was considered to be indicative of significance.

Table 2
Detection and parameters of ictal high frequency oscillations in 19 patients.

Patient	Seizure onset zone	Number of seizures	Electrodes detecting HFO	Frequency (Hz)	Amplitude (μV)	Duration (ms)	Inter-HFO Interval (s)	Total duration (s)	Time lag to EEG onset (s)
1	Lt MT (LA1-2, LH1-3, LBA1-2, LBP1-2)	3	LH1-3	200–250	25.4 (20.0–33.6)	75 (65–93)	1.15 (0.96–1.30)	30.3 (15–43)	23.2 (14–38)
2	Bil MT (RA1, RH1-2, RBP1-2, LA1-6, LH1-5, LBA1-6, LBP1-5)	3 (Rt onset)	RA1,RH1-2, RBP1	200–333	42.7 (17.8–73.2)	42 (32–61)	1.65 (1.50–1.96)	61.7 (26–91)	30.5 (8–53)
		2 (Lt onset)	RA1,RH1-2, RBP1	200–333	39.4 (18.3–71.9)	40 (35–44)	0.70 (0.60–0.80)	79.5 (70–89)	74.5 (65–84)
3	Lt MT (LBA1, LBP1)	1	LH1-3	250–333	28.7 (12.5–44.7)	27.4 (23–38)	0.37 (0.25–0.64)	71	28
4	Rt MT (RA1-2, RH1-2, RBA1-3, RBP1-3)	11	RA1	200–333	35.3 (7.4–38.2)	19 (13–37)	0.82 (0.26–1.59)	28.8 (13–63)	20 (7–27)
5	Lt MT (LA1-2, LH1-3, LBP1-2)	2	LA1-2, LBP2	200–333	27.4 (14.7–44.5)	26 (24–28)	0.60 (0.56–0.65)	41.0 (30–52)	45.0 (38–52)
6	Lt MT (LA1-2, LH1-3, LBP1-2)	3	LH2-3, LBP1	200–333	22.8 (13.5–27.1)	32 (30–33)	1.11 (0.48–1.92)	45.0 (17–75)	33.7 (24–44)
7	Rt MT (RA1-2, RH1-2)	3	RA1-2, RH1-2, LA1-2, LH1	200–333	21.6 (11.6–35.0)	27 (27–28)	1.13 (1.10–1.20)	68.3 (60–81)	28.5 (13.5–40)
				200–250	17.1 (8.8–26.8)	30 (23–36)	0.34 (0.32–0.36)	0.5 (0.36–0.64)	-3.6 (3.5–3.6)
8	Lt MT (LA1-3, LH1-3, LBP1)	6	LH2, LBP1	200–250	17.3 (13.1–21.0)	56 (19–101)	1.47 (0.74–2.14)	65.7 (19–139)	21.0 (8–40)
9	Rt MT (RA1-2, RH2-3, RBA1, RBP1-2), Rt TP	5	RA1-2	200–333	35.8 (30.9–39.7)	31 (20–47)	0.8 (0.56–1.42)	55 (29–82)	11 (6–16)
10	Rt MT (RA1-2, RH1-3, RBP1-2)	3	RA1	200–250	26.1 (16.5–35)	32 (19–64)	0.84 (0.42–1.92)	48.7 (28–80)	13.3 (12–14)
11	Rt MT (RH1-2)	2	RH1	200–250	49.3 (11.8–89.7)	28 (25–38)	1.01 (0.4–2.18)	40.5 (38–43)	5 (0–10)
12	Lt MT (LA1-2, LH1-2)	2	–	–	–	–	–	–	–
13	Rt MT (RA1-2, RBP1-2)	1	–	–	–	–	–	–	–
14	Lt basal T (LH6, LBP5-6)	2	–	–	–	–	–	–	–
15	Rt MT (RH1, RBA1, RBP1)	1	–	–	–	–	–	–	–
16	Non-localizing	3	–	–	–	–	–	–	–
17	Lt T	2	–	–	–	–	–	–	–
18	Lt hemisphere	1	–	–	–	–	–	–	–
19	Lt basal T	2	–	–	–	–	–	–	–

Lt: left; Rt: right; Bil: bilateral; MT: medial temporal; TP: temporo-parietal; T: temporal.

3. Results

3.1. Characteristics of ictal HFO

A total of 58 seizures were recorded at 1 kHz sampling rate. The seizure onset zone identified on the conventional EEG recording; number of seizures recorded at 1 kHz sampling rate; electrodes detecting HFO; frequency, amplitude and duration of HFO; inter-HFO interval; total duration; and time lag from HFO onset to EEG seizure onset are shown in Table 2. Ictal HFO were detected in 11 patients. In nine of 11 patients with HFO, all seizures recorded at 1 kHz sampling originated from the medial temporal regions ipsilateral to the side of surgical resection. In Patient 2, independent seizure onset from the left and right medial temporal regions was recorded. In Patient 9, five seizures were recorded. Three seizures originated from the right medial temporal area, while the remaining two seizures arose from the right temporo-parietal area preceding the discharges in the right medial temporal area two to 3 days after withdrawal of carbamazepine. Medial temporal onset seizures and temporo-parietal onset seizures occurred on the same day. Finally, based on all the information, including intracranial EEG findings, all 11 patients with ictal HFO in the medial temporal area were diagnosed with MTLE and underwent resection surgery. Among the remaining eight patients in whom no HFO were detected in the medial temporal structures, only three were diagnosed with MTLE (patients 12, 13, and 15), while the seizure onset zones were heterogeneous or poorly localized in the others. In one patient with no ictal HFO recorded in the medial temporal lobe (Patient 19), ictal HFO were detected in the basal temporal area (electrodes LBA5 and LBP5). Conventional ictal EEG also revealed seizure onset in the left basal temporal region (LBA3-6, LBP3-6). Basal temporal language area was also identified in the same region (LBA2-4, LBP3). This patient did not undergo resection surgery, considering the risk of language deficit.

The HFO in all 11 patients were segmental, lasted 19–75 ms (mean value), were detected in 1–4 channels, and had frequencies of 200–333 Hz. HFO could not be detected outside this frequency range. In eight of 11 patients, HFO were detected at more than one electrode. The mean amplitudes of HFO ranged from 17.3 to 49.3 μV. They were localized in unilateral medial temporal structures, mainly in the hippocampus (Fig. 2), and/or the amygdala. In three patients (patients 4, 9, and 10), ictal HFO were exclusively detected in the amygdala. HFO were also detected by subdural electrodes placed over the mediobasal temporal region (parahippocampal gyrus, TB) in five patients. HFO detected by subdural electrodes always appeared simultaneously with the HFO detected by depth electrodes. The electrodes with ipsilateral HFO were included in the seizure onset zone defined by conventional EEG in 10 patients. In the remaining patient (Patient 3), the electrodes with HFO were outside the seizure onset zone. However, both the electrodes with HFO and seizure onset zone of the patient were included in the left medial temporal structures and resected together by amygdalohippocampectomy.

HFO (ipsilateral to the side of surgical resection) onset preceded conventional EEG ictal onset by 5.0–74.5 s (mean values). The characteristics of HFO were consistent among seizures in each patient.

Ictal HFO were usually associated with spikes. When HFO were associated with spikes, they followed the peaks of the spikes. The

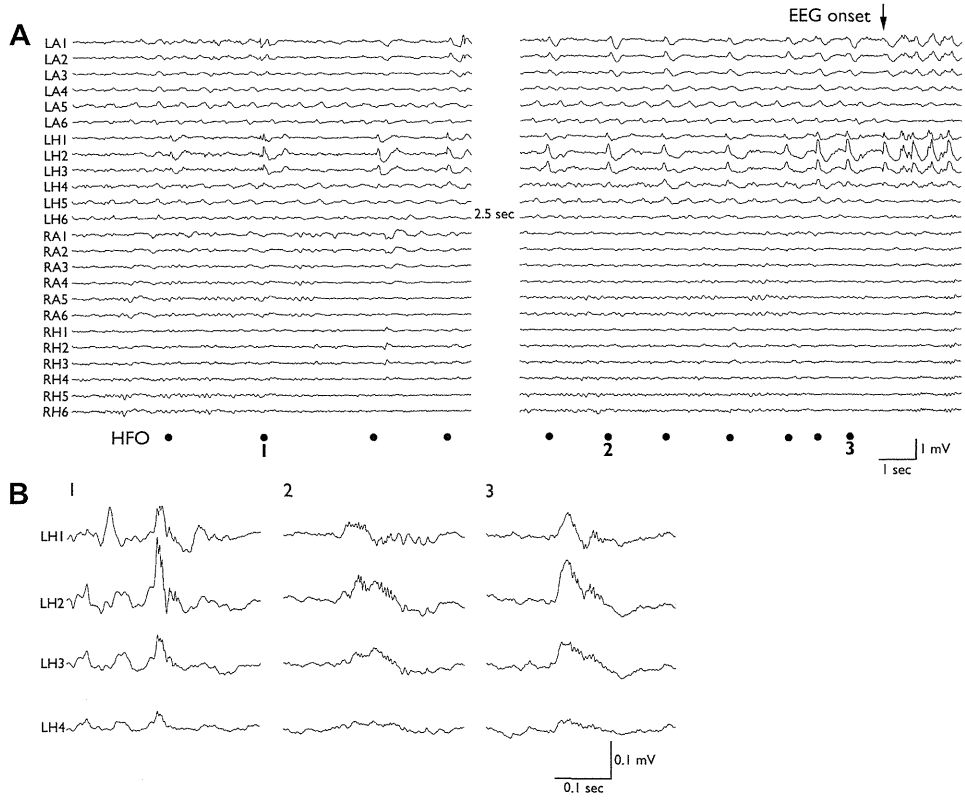

Fig. 2. Ictal EEG and HFO in Patient 1. (A) Conventional EEG (low-pass filter 120 Hz, time constant 0.1 s) reveals periodic sharp waves at LH1-3. The periodic sharp waves are followed by more repetitive sharp waves in the left hippocampus and amygdala. Filled circles indicate the presence of HFO. (B) HFO waveforms (low-pass filter 300 Hz, time constant 0.003 s). 200–250 Hz high frequency activities are detected at LH1-3. Note the calibration, which shows that HFO waves have very small amplitude and short duration.

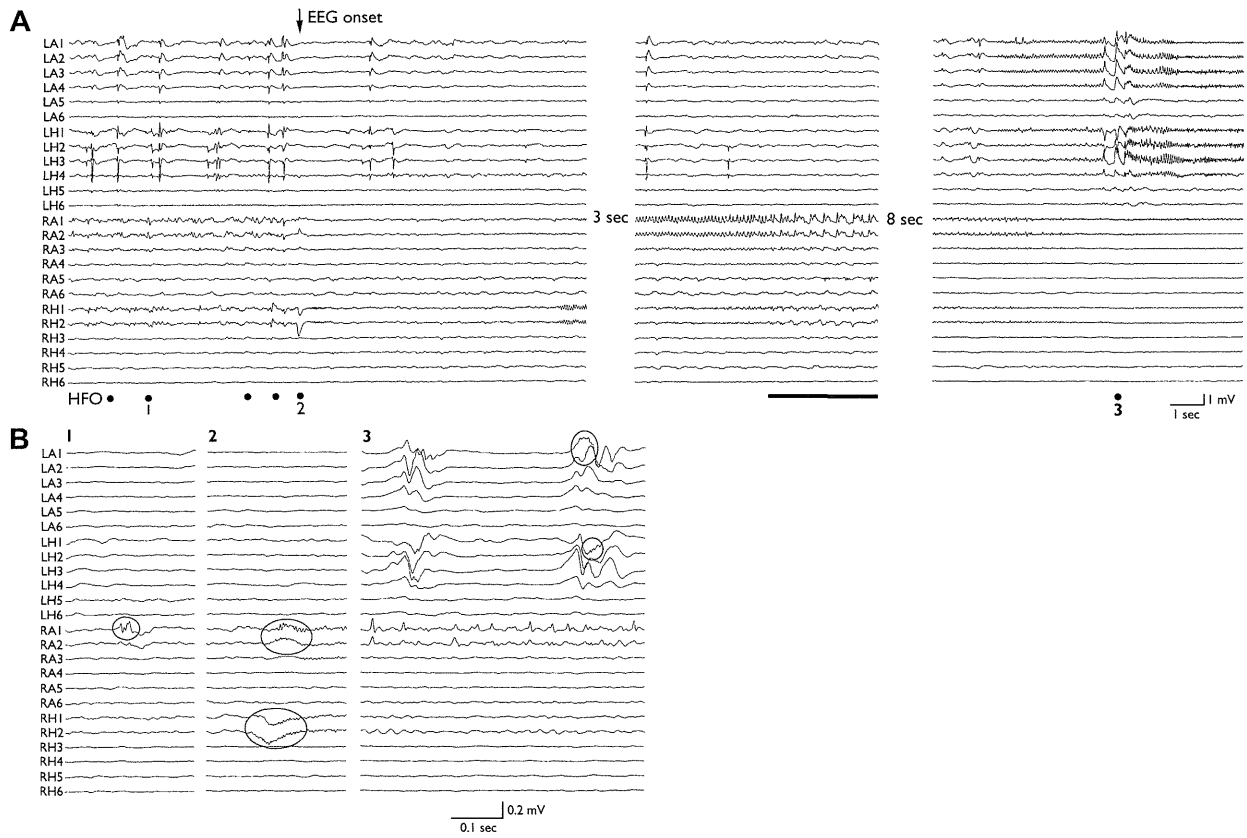

Fig. 3. Ictal EEG and HFO in Patient 7. (A) On conventional EEG (low-pass filter 120 Hz, time constant 0.1 s), ictal EEG starts with a large positive sharp wave at RH1 and RH2, followed by beta activities at the same electrodes. Seven seconds later, rhythmic beta waves start at RA1 and RA2 with gradual evolution. Approximately 45 s later, left-sided electrodes (LH1-4 and LA1-4) start showing small spikes, followed by beta activities in the same electrodes Filled circles and the bold line indicate the presence of HFO. (B) HFO waveforms before conventional EEG onset, around onset, and around conventional EEG onset at the left hemisphere (low-pass filter 300 Hz, time constant 0.003 s). These demonstrate 200–333 Hz high-frequency activities at 1–4 electrodes in the right side (RA1, RA2, RH1 and RH2). These also demonstrate high-frequency activities at LA1-2 and LH1 around the conventional EEG onset on the left side. Circles indicate the locations of HFO.

mean total duration of ictal HFO ranged from 28.8 to 79.5 s. Contralateral seizure propagation was seen in 10 of 11 patients with ictal HFO. Except for one patient (Patient 7), HFO were not detected in the areas of contralateral seizure propagation. In Patient 7, three seizures were recorded at 1 kHz sampling rate. All seizures originated from the right medial temporal region, and propagated to the left side. Ictal HFO were detected by the right medial temporal electrodes (RA1-2, RH1-2). In this exceptional case, ictal HFO were also detected in the left medial temporal electrodes (LA1-2, LH1) in two of three seizures. HFO on the left side were observed only two or three times, and the total durations of these contralateral HFO were 0.36–0.64 s, much shorter than those of HFO recorded on the resection side (Fig. 3).

In another patient (Patient 2), five seizures were recorded at 1 kHz sampling rate. On conventional EEG, three of five seizures originated from the right medial temporal region, and the remaining two from the left medial temporal region. Ictal HFO in the right medial temporal structures were observed in the three seizures originating on the right. Even in the two seizures originating from the left side, ictal HFO were detected only in the right medial temporal structures and preceded the left temporal EEG onset by 74.5 s (Fig. 4).

Interictal HFO were also detected in 10 patients (Patients 2–5, 7–11, and 18) (Table 3). These interictal HFO appeared more irregularly, and the inter-burst intervals of HFO lasted longer than those of ictal HFO. In eight patients, interictal HFO were detected only on the side of resection. In one patient (Patient 11), interictal HFO were detected in bilateral hippocampi, although the frequency of appearance was much higher on the ipsilateral side. In the remaining patient who did not proceed to surgery (Patient 18), interictal HFO were detected in the unilateral medial temporal structure.

3.2. Ictal HFO and hippocampal pathology

Surgical procedures and hippocampal pathology are shown in Table 4. In 11 patients who had ictal HFO, histological examination revealed HS in all the patients (type 1a in nine, and type 2 in two). In three patients (Patients 4, 9, and 10) showing ictal HFO exclusively in the amygdala, HS (type 1a) was also identified histologically. In eight patients who showed no ictal HFO, five underwent medial temporal resection (amygdalohippocampectomy in three, anterior temporal lobectomy including medial temporal structures in two), and pathological results were available in four of five patients. Classic sclerosis (type 1a) was observed in one patient, while no HS was found in the remaining three patients. The association between the presence of ictal HFO and HS was statistically significant ($p = 0.008791$).

3.3. Ictal HFO and postoperative seizure outcome

Favorable seizure outcome (Engel's class I) was obtained in eight of 11 patients with ictal HFO (Table 4). In one patient with class II outcome (Patient 11), a few seizures were observed soon

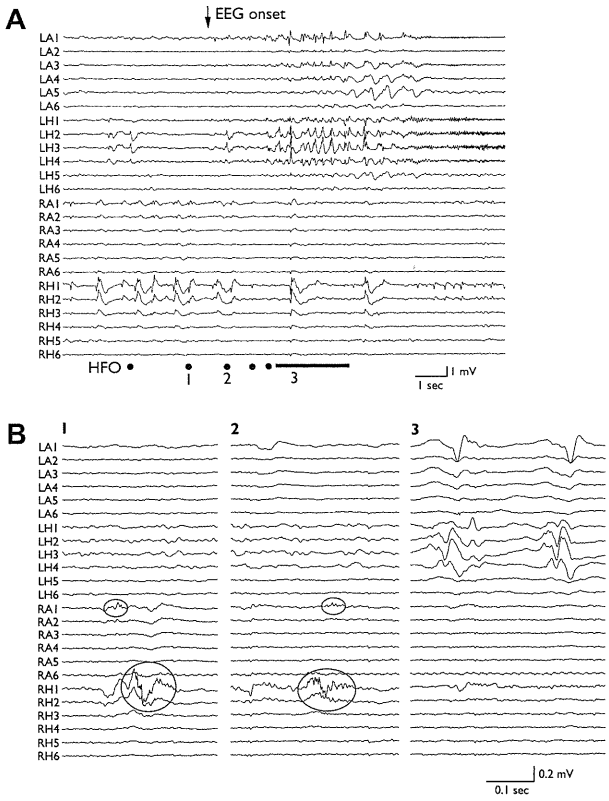

Fig. 4. Ictal EEG and HFO in Patient 2. (A) On conventional EEG (low-pass filter 120 Hz, time constant 0.1 s), ictal EEG starts with repetitive spikes at LA1, LH2, LH3, and LH4, as well as rhythmic alpha activity at LH1 at the same time. The spikes spread widely in the left temporal area, and are replaced by rhythmic beta waves at LH1, LH2, LH3, and LH4. The right hemispheric electrodes do not show clear ictal activities throughout. Filled circles and bold line indicate the presence of HFO. (B) HFO waveforms before conventional EEG onset, and around onset (low-pass filter 300 Hz, time constant 0.003 s). 200–333 Hz high frequency activities are recorded at 1 to 3 electrodes on the right side (RA1, RH1, and RH2). Circles indicate the locations of HFO. Although spikes are seen on the left side, HFO is not recorded at the left-sided electrodes.

after surgery, and the seizures were controlled by increasing antiepileptic medications. In one patient (Patient 9) with poor outcome (class III), seizures arising from contralateral temporal region were documented postoperatively. The reason for unfavorable outcome in the remaining patient (Patient 3) was unclear. Among the three cases with ictal HFO restricted to amygdala (Patients 4, 9, and 10), favorable outcome was obtained in two, and unfavorable outcome in one. Favorable seizure outcome (Engel's class I) was obtained in three of five patients without HFO who underwent resective surgery including medial temporal structures. Comparing the patients who underwent amygdalohippocampectomy in the two groups, favorable seizure outcome was obtained in seven of 10 patients with ictal HFO, and in two of three patients without HFO. Seizure outcome was not statistically different between the patients with and without ictal HFO.

4. Discussion

4.1. Characteristics of ictal HFO in medial temporal lobe

HFO in medial temporal structures have been reported in recent years. Most reports of HFO in patients with MTLE analyzed the interictal state with microelectrodes, usually during non-REM sleep (Staba et al., 2004). Fast ripples are considered to represent hypersynchronous discharges of locally interconnected principle neurons capable of generating spontaneous seizures (Staba et al., 2002). Fast ripples are most often recorded on a single microwire, supporting the hypothesis that fast ripple HFO are primarily generated by highly localized, sub-millimeter scale neuronal assembles that are most effectively sampled by microwire electrodes (Worrell et al., 2008). However, other reports have demonstrated that macroelectrodes also detect HFO in medial temporal structures (Jirsch et al., 2006; Khosravani et al., 2009; Yamaguchi et al., 2008). Although interictal HFO in the medial temporal lobe have been widely studied, the clinical significance of 'ictal' HFO in the medial temporal lobe has not been specifically studied.

In this study, multiple sites of the medial temporal regions were investigated with both depth and subdural electrodes. Ictal HFO appeared in a relatively stereotyped segmental fashion, and were detected mainly in the hippocampus and/or the amygdala. They were mostly located unilaterally ipsilateral to the side of HS, in contrast to interictal HFO in medial temporal lobe, which can be detected bilaterally (Staba et al., 2002). In eight patients, ictal HFO were detected at multiple electrode contacts, suggesting that HFO may reflect synchronous discharges widely located within unilateral medial temporal region. The sensitivity of subdural electrodes in detecting HFO was lower than that of depth electrodes.

Table 3
Detection and parameters of interictal high frequency oscillations.

Patient	Electrodes detecting HFO	Frequency (Hz)	Amplitude (μV)	Duration (ms)	Inter-HFO Interval (s)
1	None	–	–	–	–
2	RH1-2	200–333	48.5 (30.9–70.6)	31 (33–71)	24.4 (6.4–42.9)
3	LH2-3	200–333	42.7 (17.6–61.8)	25 (19–28)	1.5 (0.3–3.3)
4	RA1	200–333	25.0 (10.3–88.2)	30 (18–43)	12.1 (1.4–73)
5	LA1-2, LBP1-2	200–333	39.5 (22.6–55.8)	23 (16–32)	2.5 (0.4–17.9)
6	None	–	–	–	–
7	RA1	200–333	42.7 (20.6–85.3)	22 (13–34)	18.3 (10.6–23.7)
8	LH2, LBP1	200–250	29.4 (26.5–35.3)	50 (29–67)	4.3 (1.6–18.7)
9	RA1-2	200–333	32.0 (12.0–39.7)	25 (19–34)	2.41 (0.4–6.8)
10	RA1	200–250	29.4 (20.6–38.2)	19 (15–25)	27.8 (3.6–121)
11	RH1	200–250	57.8 (44.1–76.5)	26 (10–46)	4.3 (0.8–16.3)
	LH2	200–250	35.3 (26.5–44.1)	20 (17–23)	90 (40–199)
12	None	–	–	–	–
13	None	–	–	–	–
14	None	–	–	–	–
15	None	–	–	–	–
16	None	–	–	–	–
17	None	–	–	–	–
18	LH1–2, LBP1–2	200–333	26.8 (13.2–41.2)	27 (22–32)	31 (1–131)
19	None	–	–	–	–

Table 4
Surgery, hippocampal pathology, and seizure outcome in 19 patients.

Patient	Surgery	Follow-up (months)	MRI	Pathology (Blűmcke)	Outcome (Engel)
1	Lt AHE	49	Lt HS	HS (Type 1a)	Ia
2	Rt AHE	51	Rt HS	HS (Type 1a)	Id
3	Lt AHE	13	Lt HS	HS (Type 1a)	IIIa
4	Rt AHE	43	Rt HS	HS (Type 1a)	Ic
5	Lt ATL	33	Lt HS	HS (Type 1a)	Id
6	Lt AHE	12	Lt HS	HS (Type 2)	Ia
7	Rt AHE	22	Rt HS	HS (Type 2)	Ia
8	Lt AHE	26	Lt HS	HS (Type 1a)	Ib
9	Rt AHE	24	Rt HS	HS (Type 1a)	IIIa
10	Rt AHE	12	Rt HS	HS (Type 1a)	Ia
11	Rt AHE	17	Normal	HS (Type 1a)	IIb
12	Lt AHE	54	Normal	No HS	IIb
13	Rt AHE	35	Rt AH	No HS	Ia
14	Lt LTR	37	Normal	NA	IIIa
15	Rt AHE	48	Rt HS	HS (Type 1a)	Ic
16	Lt ATL	40	Normal	No HS	Ia
17	Lt ATL	24	Normal	NA	IIIa
18	No	–	Lt HS	–	–
19	No	–	Normal	–	–

Rt: right; Lt: left; AHE: amygdalohippocampectomy; ATL: anterior temporal lobectomy; LTR: lateral temporal resection; HS: hippocampal sclerosis; AH: amygdalar hypertrophy; NA: data not available.

Depth electrodes were inserted into subiculum, Ammon's horn, and amygdala, whereas subdural electrodes were implanted over the parahippocampal gyrus. One reason for the different sensitivity may be the different locations of the electrodes. Subiculum, Ammon's horn, and amygdala may generate ictal HFO more frequently than parahippocampal areas. Another reason may be the wider contact surface of subdural electrode (4.15 mm^2) than that of depth electrode (2.6 mm^2, calculated from the diameter and the length). In addition to the location of electrodes, the difference in contact surface of the electrodes may affect the sensitivity.

In 10 of 11 patients with ictal HFO, the electrodes with ipsilateral ictal HFO were included in the seizure onset zone, whereas in the remaining patient, they were outside the seizure onset zone. Since both the areas with HFO and seizure onset zone were resected, whether HFO or seizure onset zone is superior for deciding the area of resection cannot be determined.

Usually, HFO followed the peaks of the spikes. In a separate study of neocortical epilepsy, we found that very high frequency activities faster than 1000 Hz usually preceded the spikes. In other words, spikes seem to interrupt very high frequency activities in neocortical epilepsy. Therefore, we speculate that spikes may be an inhibitory phenomenon in neocortical epilepsy (Usui et al., 2010). On the contrary, the temporal relation between spikes and HFO in the medial temporal lobe suggests that the spikes may trigger HFO. Therefore, spikes may be an excitatory phenomenon in MTLE.

In a conventional EEG setting, inter-observer differences are common even for the interpretation of ictal onset, since conventional EEG waveforms can be very variable. On the contrary, the characteristics of medial temporal ictal HFO were very consistent among patients. Therefore, the identification of ictal HFO may support interpretation of ictal EEG.

Ictal HFO (ipsilateral to the side of surgical resection) always appeared before conventional EEG seizure onset. Except in one patient, ictal HFO did not appear in the region of contralateral spread. Moreover, they did not spread outside the medial temporal regions. These findings suggest that HFO are strongly related to epileptogenicity. Jirsch et al. (2006) also reported concordant results. In one exceptional case, HFO appeared in the area of contralateral seizure spread, but the total duration of contralateral HFO was much shorter. In this case, amygdalohippocampectomy on the side of seizure origin was performed, and the patient has been seizure free for approximately 2 years. Careful follow-up of this patient is necessary to evaluate epileptogenicity in the contralateral medial temporal lobe.

Temporal lobe epilepsy has been considered as a bilateral disease (Margerison and Corsellis, 1966). It is often difficult to decide the surgical indication and the side of resection in patients with bitemporal epilepsy, even with intracranial EEG. In one patient, clinical seizures originated independently from bilateral medial temporal lobes when assessed on conventional EEG. However, ictal HFO were detected unilaterally. The findings in this patient strongly suggest that ictal HFO may not be just a part of ictal EEG changes, but probably represent electrophysiological phenomena independent of the activity usually detected by conventional EEG, and that epileptogenicity and ictogenicity could be differentiated by ictal HFO. Crépon et al. (2010) recently studied interictal HFO with macroelectrodes, and reported detection of interictal HFO unilaterally in a case of bitemporal seizure onset. They suggested the usefulness of interictal HFO for defining the seizure onset zone. In our patients, interictal HFO were detected in 10 patients, and they were unilateral and ipsilateral to the side of resection in eight patients. Therefore, interictal HFO may be also useful for deciding the side of resection. However, interictal HFO in medial temporal lobe has also been detected bilaterally (Staba et al., 2002). The one reason for disagreement may be the extended periods of recording in the study by Staba et al. (2002) (the mean length of time analyzed was 177 ± 7 min of non-REM sleep) compared with our study (5 min). Further studies are necessary for clarifying the usefulness of ictal and interictal HFO for deciding the side of resection in bitemporal epilepsy.

4.2. Correlation with hippocampal pathology

Using microelectrodes, Staba et al. (2007) reported that higher fast ripples to ripple ratios are associated with histopathologic changes found in HS in TLE patients. Recently, Ogren et al. (2009) studied interictal HFO recorded by hippocampal microelectrodes in 10 patients with MTLE, and demonstrated the proximity between fast ripples and local hippocampal atrophy. Our study demonstrated a strong association between ictal HFO (fast ripple range) in medial temporal lobe detected by macroelectrodes and HS. In Patient 11, preoperative MRI did not reveal clear HS. However, ictal HFO were detected in the right hippocampal electrode and HS was detected pathologically. Ictal HFO in the medial temporal lobe may be the electrophysiological signature of HS. Neuron loss and synaptic reorganization may contribute to the generation of HFO (Ogren et al., 2009).

Among the four patients without ictal HFO who underwent resection of the medial temporal lobe, histopathology revealed no HS in three of four patients. In Patient 13 with no HS, amygdalohippocampectomy was performed and the patient became seizure free. Ictal HFO may be absent in patients with MTLE without HS. In one patient who had HS (classic sclerosis) but no HFO (Patient 15), seizures continued with somatomotor signs for 2 years after amygdalohippocampectomy, and then became controlled without medication adjustment, and she has been seizure-free for more than 2 years (Engel's class Ic). Although the reason for late seizure remission in this patient is not clear, the epileptogenic zone might not be restricted to medial temporal structures. In addition to HS, primary epileptogenicity in the medial temporal lobe may be a requisite for generating ictal HFO.

4.3. Correlation with postoperative seizure outcome

Eight of 11 patients with HFO achieved Engel's class I outcome, and one patient had class II outcome. In one case (Patient 9), contralateral temporal onset seizures were recorded after surgery, although contralateral HFO was never recorded during invasive monitoring. Although an association between resection of ictal HFO generating zone and favorable seizure outcome in neocortical epilepsy has been suggested (Ochi et al., 2007), such a relationship could not be proven in this study. However, this result should be interpreted with caution. A strong association with ictal HFO and HS was established in this study. All patients with ictal HFO were diagnosed with MTLE. Subsequently, seven of 10 patients with HFO who underwent amygdalohippocampectomy obtained good seizure outcome. On the contrary, only three of eight patients without HFO were diagnosed with MTLE. In other patients, the epileptogenic zone was heterogeneous or poorly localized. The presence of ictal HFO in the medial temporal lobe strongly favors a diagnosis of MTLE with HS and subsequent resective surgery. The small number of patients without HFO may lead to the negative result for seizure outcome. Further study including more patients without HFO may clarify the relationship between the presence of ictal HFO and postoperative seizure outcome.

Jacobs et al. (2010) analyzed interictal HFO in 20 patients, and compared rates and extents of HFO in resected and non-resected areas with surgical outcome. Patients with a good outcome (Class I or II) had a significantly larger proportion of HFO-generating areas removed than patients with a poor outcome (Class III or IV). In our 11 patients with ictal HFO, HFO-generating areas were completely resected in all 11 patients. However, there were two patients with a poor outcome (Class III). The discordance may be due to the fact that Jacobs et al. included both fast ripples and ripples as HFO, whereas we did not include ripples as HFO. Ripples can be either pathologic or memory-related. Further studies for differentiating pathological ripples from healthy, memory-related ones are necessary.

4.4. Clinical significance of absence of HFO in the medial temporal lobe

In eight patients, no ictal HFO was detected in the medial temporal lobe. Compared to patients with HFO, the epileptogenic zones of patients without HFO were more heterogeneous or poorly localized.

When no ictal HFO is detected in the medial temporal area, two possibilities should be considered. One is that the diagnosis is not MTLE. In Patient 16, lateral temporal lobe epilepsy was diagnosed and left anterior temporal lobectomy, including medial temporal lobe, was performed with complete seizure control, and histopathology revealed no HS. In this case, absence of ictal HFO in the medial temporal lobe may simply reflect that the medial temporal lobe might not be included in the epileptogenic zone. In Patient 19 with no HFO in the medial temporal lobe, ictal HFO were detected in the basal temporal lobe. Ictal high frequency activities recorded from neocortex have been reported (Jirsch et al., 2006; Ochi et al., 2007; Usui et al., 2010). However, most of the patients in this study were diagnosed with possible temporal lobe epilepsy. Therefore neocortical HFO was not common. Another possibility is that the diagnosis is MTLE without HS. In Patient 13, amygdalohippocampectomy resulted in seizure control, and histopathology revealed no HS. Therefore, in some patients with MTLE without HS, ictal HFO may not be detected. Although further research is needed, ictal HFO in the medial temporal lobe may be a specific marker for MTLE with HS.

References

Blűmcke I, Pauli E, Clusmann H, Schramm J, Becker A, Elger C, Merschhemke M, Meencke H, Lehmann T, Von Deimling A, Scheiwe C, Zentner J, Volk B, Romstőck J, Stefan H, Hildebrandt M. A new clinico-pathological classification system for mesial temporal sclerosis. Acta Neuropathol. 2007;113:235–44.

Bragin A, Engel J, Wilson CL, Fried I, Buzsáki G. High-frequency oscillations in human brain. Hippocampus 1999;9:137–42.

Bragin A, Wilson CL, Staba RJ, Reddick M, Fried I, Engel Jr J. Interictal high-frequency oscillations (80–500 Hz) in the human epileptic brain: entorhinal cortex. Ann. Neurol. 2002;52:407–15.

Crépon B, Navarro V, Hasboun D, Clemenceau S, Martinerie J, Baulac M, Adam C, Le Van Quyen M. Mapping interictal oscillations greater than 200 Hz recorded with intracranial macroelectrodes in human epilepsy. Brain 2010;133:33–45.

Gastaut H., Fischer-Williams, M. The physiopathology of epileptic seizures. American Physiological Society, Handbook of Physiology: A critical, comprehensive presentation of physiological knowledge and concepts. American Physiological Society, Washington DC, 1959, pp. 329–363.

Jacobs J, Zijlmans M, Zelmann R, Chatillon C-E, Hall J, Olivier A, Dubeau F, Gotman J. High-frequency electroencephalographic oscillations correlate with outcome of epilepsy surgery. Ann. Neurol. 2010;67:209–20.

Jirsch JD, Urrestarazu E, Levan P, Olivier A, Dubeau F, Gotman J. High-frequency oscillations during human focal seizures. Brain 2006;129:1593–608.

Khosravani H, Mehrotra N, Rigby M, Hader W, Pinnegar CR, Pillay N, Wiebe S, Federico P. Spatial localization and time-dependent changes of electrographic high frequency oscillations in human temporal lobe epilepsy. Epilepsia 2009;50:605–16.

Lüders H, Acharya J, Baumgartner C, Benbadis S, Bleasel A, Burgess R, Dinner DS, Ebner A, Foldvary N, Geller E, Hamer H, Holthausen H, Kotagal P, Morris H, Meencke HJ, Noachtar S, Rosenow F, Sakamoto A, Steinhoff BJ, Tuxhorn I, Wyllie E. Semiological seizure classification. Epilepsia 1998;39:1006–13.

Margerison JH, Corsellis JAN. Epilepsy in the temporal lobes. Brain 1966;89:499–530.

Mihara T, Baba K. Combined use of subdural and depth electrodes. In: Lűders HO, Comair YG, editors. Epilepsy surgery. second ed. Philadelphia: Lippincott Williams & Wilkins; 2001. p. 613–21.

Mihara T, Matsuda K, Tottori T, Baba K, Inoue Y, Hiyoshi T, Watanabe Y, Yagi K, Seino M. Conditions for omitting intracranial long-term monitoring before surgical resection in patients with temporal lobe epilepsy. Jpn. J. Psychiatry Neurol. 1992;46:323–9.

Ochi A, Otsubo H, Donner EJ, Elliott I, Iwata R, Funaki T, Akizuki Y, Akiyama T, Imai K, Rutka JT, Snead III OC. Dynamic changes of ictal high-frequency oscillations in neocortical epilepsy: using multiple band frequency analysis. Epilepsia 2007;48:286–96.

Ogren JA, Wilson CL, Bragin A, Lin JJ, Salamon N, Dutton RA, Luders E, Fields TA, Fried I, Toga AW, Thompson PM, Engel Jr J, Staba RJ. Three-dimensional surface maps link local atrophy and fast ripples in human epileptic hippocampus. Ann. Neurol. 2009;66:783–91.

Spencer SS, Guimaraes P, Katz A, Kim J, Spencer D. Morphological patterns of seizures recorded intracranially. Epilepsia 1992;33:537–45.

Staba RJ, Wilson CL, Bragin A, Fried I, Engel Jr J. Quantitative analysis of high-frequency oscillations (80–250 Hz) recorded in human epileptic hippocampus and entorhinal cortex. J. Neurophysiol. 2002;88:1743–52.

Staba RJ, Wilson CL, Bragin A, Jhung D, Fried I, Engel Jr J. High-frequency oscillations recorded in human medial temporal lobe during sleep. Ann. Neurol. 2004;56:108–15.

Staba RJ, Frighetto L, Behnke E, Mathern GW, Fields T, Bragin A, Ogren J, Fried I, Wilson CL, Engel Jr J. Increased fast ripple to ripple ratios correlate with reduced hippocampal volumes and neuron loss in temporal lobe epilepsy patients. Epilepsia 2007;48:2130–8.

Usui N, Terada K, Baba K, Matsuda K, Nakamura F, Usui K, Tottori T, Umeoka S, Fujitani S, Mihara T, Inoue Y. Very high frequency oscillations (over 1000 Hz) in human epilepsy. Clin. Neurophysiol. 2010;121:1825–31.

Worrell GA, Gardner AB, Stead SM, Hu S, Goerss S, Cascino GJ, Meyer FB, Marsh R, Litt B. High-frequency oscillations in human temporal lobe: simultaneous microwire and clinical macroelectrode recordings. Brain 2008;131:928–37.

Yamaguchi M, Terada K, Baba K, Nakamura F, Inoue Y. Ictal high frequency oscillations in patients with mesial temporal lobe epilepsy. Jpn. J. Clin. Neurophysiol. 2008;36:615–23.

VOLUME 69, ISSUE 1 JANUARY 2011

ANNALS of Neurology

JOURNAL OF THE AMERICAN NEUROLOGICAL ASSOCIATION AND THE CHILD NEUROLOGY SOCIETY

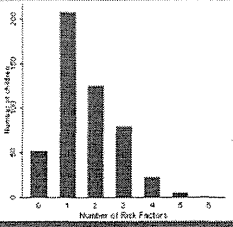

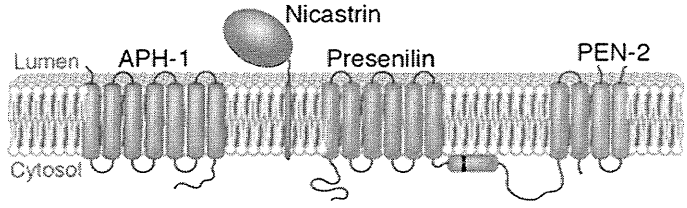

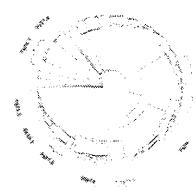

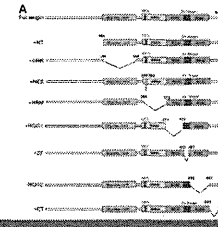

WILEY-BLACKWELL

ISSN 0364-5134

therefore, a diagnosis of exclusion because a disease morphological marker in the peripheral nerve is still lacking. However, a definite diagnosis of MN is possible.

The biopsy of the motor branch of the obturator nerve should be considered as a potential diagnostic tool for early differential diagnosis of selected cases of LMND and MN.

Acknowledgments

This research was supported by Istituto Superiore di Sanità e Fondo per gli investimenti della Ricerca di Base TissueNet (to A.Q.) and by MoH RF-FSR-2007-637144 to S.I.

Potential Conflict of Interest

Nothing to report.

References

1. Carus R. Motor neurone disease: a demeaning illness. Br Med J 1980;280:455–456.
2. de Carvalho M, Dengler R, Eisen A, et al. Electrodiagnostic criteria for diagnosis of ALS. Clin Neurophysiol 2008,119:497–503.
3. Brooks BR, Miller RG, Swash M, Munsat TL. World Federation of Neurology Research Group on Motor Neuron Diseases. El Escorial revisited: revised criteria for the diagnosis of amyotrophic lateral sclerosis. Amyotroph Lateral Scler Other Motor Neuron Disord 2000;1:293–300.
4. Van den Berg-Vos RM, Visser J, Kalmijn S, et al. A long-term prospective study of the natural course of sporadic adult-onset lower motor neuron syndromes. Arch Neurol 2009;66:751–757.
5. Visser J, van den Berg-Vos RM, Franssen H, et al. Mimic syndromes in sporadic cases of progressive spinal muscular atrophy. Neurology 2002;58:1593–1596.
6. Scottish Motor Neuron Disease Research Group. The Scottish Motor Neuron Disease Register: a prospective study of adult onset motor neuron disease in Scotland. Methodology, demography and clinical features of incident cases in 1989. J Neurol Neurosurg Psychiatry 1992;55:536–541.
7. Davenport RJ, Swingler RJ, Chancellor AM, Warlow CP. Avoiding false positive diagnoses in motor neuron disease: lessons from the Scottish Motor Neuron Disease Register. J Neurol Neurosurg Psychiatry 1996;60:147–151.
8. Traynor BJ, Codd MB, Corr B, et al. Clinical features of amyotrophic lateral sclerosis according to the El Escorial and Airlie House diagnostic criteria. Arch Neurol 2000;57:1171–1176.
9. Van Asseldonk JT, Franssen H, Van den Berg-Vos RM, et al. Multifocal motor neuropathy. Lancet Neurol 2005;4:309–319.
10. Katz JS, Barohn RJ, Kojan S, et al. Axonal multifocal motor neuropathy without conduction block or other features of demyelination. Neurology 2002;58:615–620.
11. Delmont E, Azulay JP, Giorgi R, et al. Multifocal motor neuropathy with and without conduction block: a single entity? Neurology 2006;67:592–596.
12. Shook SJ, Pioro EP. Racing against the clock: recognizing, differentiating, diagnosing, and referring the amyotrophic lateral sclerosis patient. Ann Neurol 2009;65:S10–S16.
13. Corbo M, Abouzahr MK, Latov N, et al. Motor nerve biopsy studies in motor neuropathy and motor neuron disease. Muscle Nerve 1997;20:15–21.
14. Dubowitz V, Sewry CA. Neurogenic disorders. In: Dubowitz V, Sewry CA, eds. Muscle biopsy. A practical approach. 3th ed. Philadelphia: Elsevier Saunders, 2007:275–292.
15. Dick PJ, Dyck PJB, Engelstad J. Pathologic alterations of nerves. In: Dyck PJ, Thomas PK, eds. Peripheral neuropathy. 4th ed. Philadelphia: Elsevier Saunders, 2005:733–830.
16. Previtali SC, Malaguti MC, Riva N, et al. The extracellular matrix affects axonal regeneration in peripheral neuropathies. Neurology 2008;71:322–331.
17. Grant IA, Benstead TJ. Differential diagnosis of polineuropathy. In: Dyck PJ, Thomas PK, eds. Peripheral neuropathy. 4th ed. Philadelphia: Elsevier Saunders. 2005:1163–1180.
18. Atsumi T. The ultrastructure of intramuscular nerves in amyotrophic lateral sclerosis. Acta Neuropathol 1981;55:193–198.
19. Mitsumoto H, Chad DA, Pioro EP. Neuropathology. In: Amyotrophic lateral sclerosis. Philadelphia: FA Davis Company, 1998:179–196.
20. Taylor BV, Dyck PJ, Engelstad J, et al. Multifocal motor neuropathy: pathologic alterations at the site of conduction block. J Neuropathol Exp Neurol 2004;63:129–137.

Ictal Very Low Frequency Oscillation in Human Epilepsy Patients

Liankun Ren, MD,[1,2] Kiyohito Terada, MD,[2] Koichi Baba, MD,[3] Naotaka Usui, MD,[3] Shuichi Umeoka, MD,[3] Keiko Usui, MD,[2] Kazumi Matsuda, MD,[3] Takayasu Tottori, MD,[3] Fumihiro Nakamura, MD,[4] Tadahiro Mihara, MD,[3] and Yushi Inoue, MD[4]

Using intracranial electroencephalographic recordings, we identified a distinct brain activity in 3 patients with refractory epilepsy characterized by very early occurrence from 8 minutes 10 seconds to 22 minutes 40 seconds prior to clinical seizure onset, periodical appearance of slow negative baseline shift, long interpeak interval of 40 to 120 seconds, and disappearance after clinical seizure. We named this activity "very low frequency oscillation" (VLFO), which reflected a dynamic process during the preictal state.

From the [1]Department of Neurology, China-Japan Friendship Hospital, Beijing, China; and Departments of [2]Neurology, [3]Neurosurgery, and [4]Psychiatry, National Epilepsy Center, Shizuoka Institute of Epilepsy and Neurological Disorders, Aoi-ku, Shizuoka, Japan.

Address correspondence to Dr Terada, Department of Neurology, National Epilepsy Center, Shizuoka Institute of Epilepsy and Neurological Disorders, 886 Urushiyama, Aoi-ku, Shizuoka, 420-8688 Japan. E-mail: kyht-terada@umin.net

Additional Supporting Information can be found in the online version of this article.

Received Mar 14, 2010, and in revised form Jun 14, 2010. Accepted for publication Jul 9, 2010.

View this article online at wileyonlinelibrary.com. DOI: 10.1002/ana.22158

This observation may render new insight into epileptogenesis and provide additional information concerning the epileptogenic zone as well as prediction of epileptic seizures.

ANN NEUROL 2011;69:201-206

Electroencephalography (EEG) is essential for assessing patients with epilepsy. Conventionally, EEG is usually analyzed at a narrow frequency band ranging from 0.5Hz to 70Hz. However, brain activities beyond the conventional frequency range, such as high-frequency oscillation (HFO) ranging from 100Hz to 500Hz,[1,2] very high frequency oscillation (VHFO)[3] (over 1,000Hz), infraslow brain activity,[4] and ictal direct current shift (IDS)[5] have also been observed. In recent years, these unconventional EEG findings have remained a topic of intensive investigation for their clinical significance.

We first report here a distinct ictal electrophysiological activity in the infraslow band, which was detected in 3 patients with refractory neocortical epilepsy by means of subdural electrodes. It was characterized by very early occurrence before the clinical seizure onsets, periodical appearance of slow negative baseline shifts, gradual evolution in amplitude, frequency, and distribution, and disappearance soon after the clinical seizures. Since it was distinguishable from any previously known ictal EEG patterns, we named it "ictal very low frequency oscillation" (VLFO) to highlight its unique neurophysiological features.

Patients and Methods

We investigated 26 patients with intractable neocortical epilepsy who underwent presurgical evaluation with subdural electrodes because noninvasive investigations could not delineate their epileptogenic zone (EZ), between July 2004 and June 2009 at the Shizuoka Institute of Epilepsy and Neurological Disorders. A low-frequency filter of 0.016Hz, which was in accordance with a time constant (TC) of 10 seconds was used during recording in these patients.

We used a digital EEG machine (Neurofax, Nihon-Koden Corp., Tokyo, Japan). The invasive electrodes were placed according to the clues indicated by noninvasive studies. Each subdural electrode was 2.3mm in diameter, linearly arrayed, made of platinum-iridium alloy, and with a center-to-center electrode distance of 10mm (Ad-Tech Medical Instrument Corp., Racine, WI). Recording sessions started 1 week after the implantation of electrodes, and lasted for 2 weeks.

The parameters for the conventional analysis of EEG are TC of 0.1 second, high frequency filter (HFF) of 70 Hz, and 10 seconds per epoch of EEG display. To pick up very slow periodic electrical potentials, we evaluated the EEG with TC of 10 seconds and a highly compacted EEG display with 5 minutes per epoch (30 times the routine EEG display). For each patient, a 2-hour EEG window with 1 hour before and 1 hour after the clinical seizures, and 5-hour continuous interictal EEG was evaluated.

Results

Among 26 patients, only 3 patients clearly demonstrated VLFO (Figs 1–3, Supporting Fig S1D, and Supporting Figs S2–S4). Patient 1 was an 18-year-old female, having drug-resistant seizures including simple partial seizures (SPS) manifesting focal motor symptoms and secondarily generalized tonic-clonic seizures (sGTC) since 2 years of age. Her brain magnetic resonance imaging (MRI) showed increased signal intensity on the right parietal cuneus in fluid attenuation inversion recovery (FLAIR) imaging. The scalp EEG demonstrated interictal low-amplitude spikes or sharp waves over the right parietal area. Ictal discharges started with low-amplitude slow waves over the right occipital and posterior temporal areas. Patient 2 was a 30-year-old female whose seizures occurred at the age of 16 years. Her seizures, including auras manifesting as complex auditory symptoms, complex partial seizures (CPS), and sometimes followed by sGTC, were refractory to antiepilepsy drugs (AEDs). Her brain computed tomography (CT) and MRI were normal. Scalp interictal EEG showed epileptiform discharges in the left anterior temporal area, and ictal discharges started with 6Hz, theta activities over the left anterior temporal area, evolving into the surrounding areas. Patient 3 was a 23-year-old male having seizures since 12 years of age. His refractory CPS started with the eyes and head turning to the left side, sometimes followed by sGTC. Surface interictal EEG showed intermittent spikes over the right frontal, temporal, and parietal lobes dependently, while diffuse ictal discharges were found widely over the right hemisphere. His brain MRI showed mild increased signal intensity in the right frontal inferior sulcus in FLAIR imaging (see Fig 3).

During intracranial EEG monitoring, 9 SPS and 7 sGTC in Patient 1; 2 SPS, 4 CPS, and 2 sGTC in Patient 2; and 4 CPS and 11 sGTC in Patient 3 were captured and analyzed in total.

With highly compacted EEG display and long TC of 10 seconds, very slow, irregular, low-amplitude baseline fluctuations were found during the interictal period. However, there was no regular, periodic, or evolving pattern (see Supporting Fig S1B). In contrast, VLFO were clearly identified only prior to CPS (8/8 seizures) and sGTC (20/20 seizures) but not SPS (0/11 seizures) in these 3 patients. The pattern of VLFO was homogenous, but with variation of time duration and amplitude

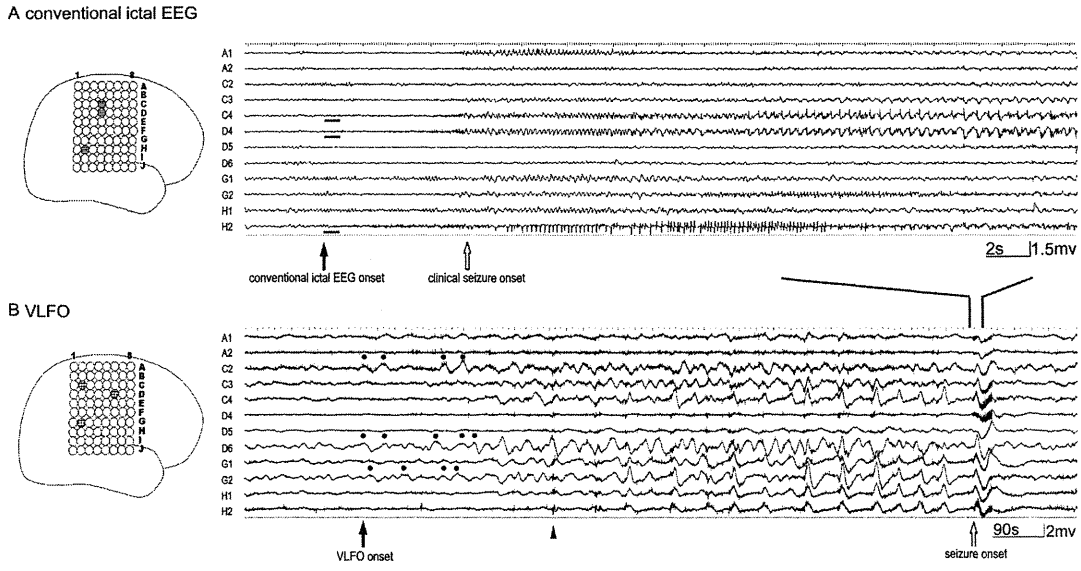

FIGURE 1: Ictal EEG changes during one sGTC with schematic location of electrodes in Patient 1. (A) Conventional ictal discharges (a TC of 0.1 second, HFF 70Hz) started with low amplitude, followed by fast activities originating from C4, D4, and H2 *(black arrow and bold lines)* 6 seconds before clinical onset *(white arrow)*. (B) VLFO (a TC of 10 seconds, HFF 70 Hz, highly compacted display) developed over C2, D6, and G2 *(black dots)*, followed by gradual evolution in morphology, amplitude, frequency, and wider distribution. A particularly well-organized periodic pattern developed with an interpeak interval from 40 to 60 seconds over C4, G1, G2, H1, and H2. The maximal amplitude became more than 3mV. The onset of VLFO *(black arrow)* preceded clinical seizure onset *(white arrow)* by 18 minutes 10 seconds. Notably, positive IDS could be detected in the initial stage of seizure onset on A1, A2, D4, and D5, channels in which VLFO was insignificant. The *black triangle* marks enhanced interictal discharges, which were superimposed over VLFO. The *open frame of black lines* indicates the time window in A.

among seizures in individual patients. No subjective complaints or objective symptoms were reported during VLFO. The observation of the interictal discharges, conventional ictal EEG, VLFO, and cortical mapping are summarized in Supporting Table S1.

VLFO in 3 patients shared common essential features: (1) The occurrence always preceded clinical seizure onset and conventional ictal EEG onset by a period of time ranging from 8 minutes 10 seconds to 22 minutes 40 seconds. Gradually, repetitive negative slow baseline shifts developed from very limited areas involving a few electrodes. (2) The morphology, amplitude, frequency, and distribution of VLFO evolved progressively. Generally, VLFO became more regular and periodical. Interpeak intervals of 40–120 seconds and more than 3mV of maximal amplitudes were detected. (3) The intensive interictal discharges in Patient 1 and subclinical discharge in Patient 2 were superimposed on the VLFO waveform several minutes after VLFO occurrence. (4) The spatial distributions of VLFO were in the vicinity of, or even overlapped with the conventional ictal EEG onset and IDS. (5) Finally, VLFO disappeared or significantly attenuated after cessation of the clinical seizure.

Patients 1 and 2 were not operated on because the EZ could not be localized clearly and/or the eloquent areas overlapped with the possible EZ. Patient 3 underwent lesionectomy (see Supporting Fig 1C). The lesion was confirmed as focal cortical dysplasia histologically. His seizures reduced by about 50%, although the follow-up period is still less than 1 year.

Discussion

The current study revealed a distinct ictal brain activity in the range of the infraslow band. Theoretically, if EEG recording is carried out with direct current (DC) amplification or alternate current (AC) amplification, but with very long TC, slow potentials can be evaluated.[6] Nevertheless, significant artifacts in surface EEG, the routinely-used short TC, or unavailability of a DC amplifier made it difficult or even impossible to observe DC shift. Intracranial recording, very long TC, and highly compacted EEG display were necessary to identify VLFO. The platinum-iridium alloy electrodes are optimal to minimize electrode potentials, which could distort slow potential signals.[7] It is essential to differentiate real activities from artifacts resulting from electrode placement, patient movements, or other noise in the evaluation of VLFO. Artifacts are readily detected based on irregularity or bizarre morphology, long-lasting instability of the

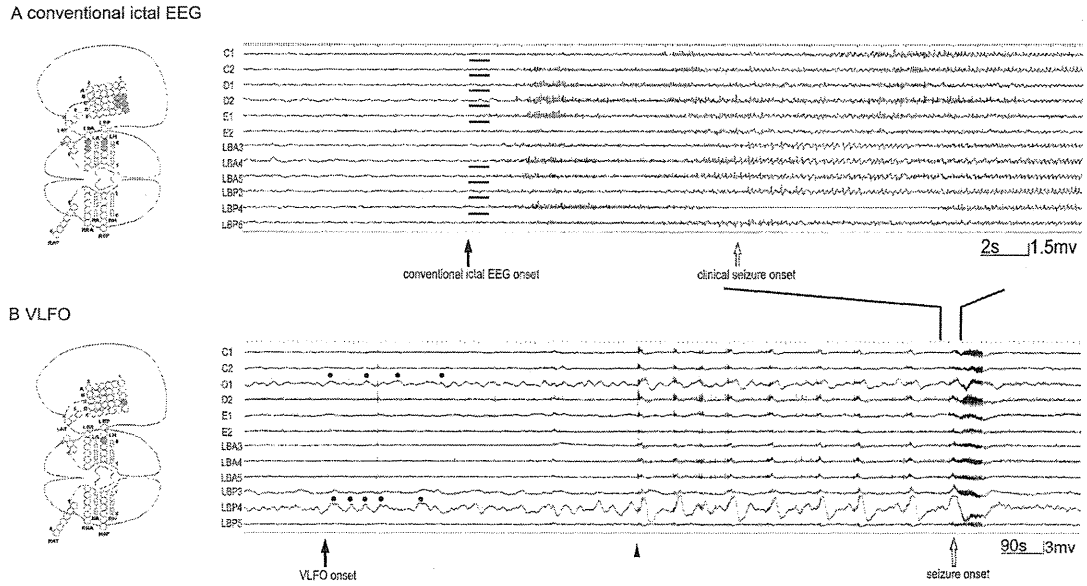

FIGURE 2: Ictal EEG changes during 1 CPS with schematic location of electrodes in Patient 2. (A) Conventional ictal discharges (a TC of 0.1 seconds, HFF 70Hz) started with low-amplitude fast activity *(black arrow and bold lines)* 12 seconds before clinical onset *(white arrow)* over the basal temporal and posterior lateral temporal lobes simultaneously. (B) VLFO (a TC of 10 seconds, HFF 70 Hz, highly compacted display) developed at LBP4 and D1 *(black dots)*, evolving into a higher-amplitude and well- organized periodic pattern with interpeak interval from 90 to 120 seconds. The maximal amplitude became more than 3mV. The onset of VLFO *(black arrow)* preceded clinical seizure onset *(white arrow)* by 22 minutes 40 seconds. The *black triangle* indicates onset of subclinical discharges, which were superimposed over VLFO. The *open frame of black lines* indicates the time window in A.

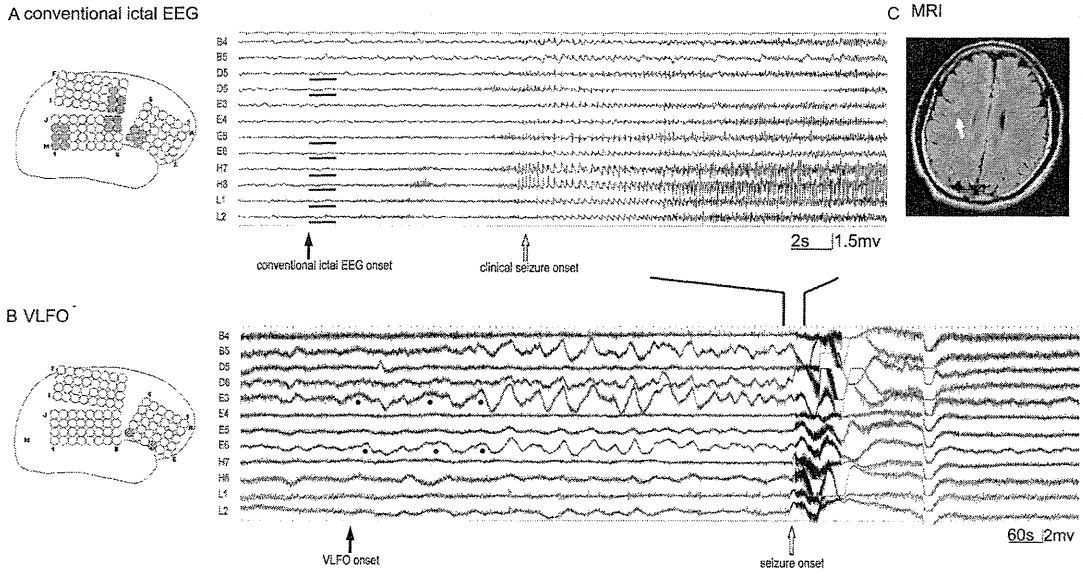

FIGURE 3: Ictal EEG changes during one sGTC with schematic location of electrodes in Patient 3. (A) Conventional ictal EEG (a TC of 0.1 seconds, HFF 70Hz) started with low-voltage fast activities regionally 10 seconds prior to clinical onset *(white arrow)* in a start-attenuation-restart pattern *(black arrow and bold lines)*. (B) VLFO (a TC of 10 seconds, HFF 70 Hz, highly compacted display) developed at E3 and E6 *(black dots)*, becoming higher, wider, and periodic, and disappeared with seizure cessation. A particularly well-organized periodic pattern developed with an interpeak interval from 40 to 60 seconds over B5, E3, and E6. Clearly, negative IDS could be identified in the initial stage of seizure onset over E5, H7, H8, L1, and L2, channels in which VLFO was insignificant. VLFO onset *(black arrow)* preceded clinical seizure onset *(white arrow)* by 13 minutes 20 seconds. The *open frame of black lines* indicates the time window in A. (C) MRI findings demonstrated the thickness of gyrus with mildly increased signal in the right inferior frontal lobe *(white arrow)*.

baseline, lack of evolution pattern, or continuation after the seizures.

Identification of VLFO would expand the brain activity spectrum, and it is different from any other previously known slow activities. The exclusive correlation between VLFO and clinical seizure distinguish it from interictal infraslow activity,[4] which might represent the slow, cyclic modulation of cortical gross excitability. Also, it is easily distinguished from IDS, which occurred with conventional EEG onset almost simultaneously and is supposed to result from astrocytic depolarization due to the increased extracellular potassium released from the vicinity of firing neurons,[8] because of its very early appearance, periodic evolving pattern, and the discrepancy in the distribution.

The observation of VLFO would also broaden our understanding of epileptogenesis. Traditionally, epileptic physiology was neuron-centric. A 50-msec to 200-msec paroxysmal depolarization shift (PDS) was considered a hallmark of epilepsy.[9] However, epileptogenesis might be heterogeneous. The role of astrocytes is especially interesting, for they not only can exhibit excitability in the form of spontaneous calcium oscillation with an interval of up to several minutes,[10,11] but also have a complex interaction with neurons.[12,13] Astrocytes are found to express similar ion channels and receptors to neurons and release gliotransmitters, including glutamate, to act on neurons, resulting in synchronizing neuronal activity[14,15] or triggering PDS-like events.[16] Therefore, it is assumed that astrocytes might initiate the VLFO, followed by activating neurons and driving epileptiform discharges, finally resulting in clinical seizure.

VLFO may be of clinical significance for identification of reliable biological markers for EZ, since currently no single technique can point out the EZ perfectly.[17] Since VLFO was only identified with seizure, and the spatial distributions of interictal discharges, conventional ictal EEG onset, IDS and VLFO were adjacent, or even overlapped, VLFO has the potential to provide valuable additional information to determine EZ despite the limited number of patients in this study. Furthermore, VLFO provides evidence for the dynamic preictal state that has long been debated. One of the most disabling aspects of epilepsy is the unpredictability of seizures. If reliable prediction is possible, epilepsy treatment will improve dramatically.[18] Although many efforts have been made to extract preictal EEG changes from continuous EEG since the 1970s,[19] more recent studies could not reproduce previously optimistic findings.[20] Hence, the relatively long time lag between occurrence of VLFO and clinical seizure makes VLFO potentially a potent parameter for predicting seizures.

Acknowledgments

This research was supported by the Japan Epilepsy Society and the Epilepsy Research Foundation of Japan (to L.R.).

We thank Ms. Miyako Yamaguchi, and Ms. Mariko Ishikawa for technical assistance.

Potential Conflicts of Interest

Nothing to report.

References

1. Bragin A, Engel JJ, Wilson CL, et al. High-frequency oscillations in human brain. Hippocampus 1999;9:137–142.
2. Bragin A, Engel JJ, Wilson CL, et al. Hippocampal and entorhinal cortex high-frequency oscillations (100–500 Hz) in human epileptic brain and in kainic acid-treated rats with chronic seizures. Epilepsia 1999;40:127–137.
3. Usui N, Terada K, Baba K, et al. Very high frequency oscillations (over 1000 Hz) in human epilepsy. Clin Neurophysiol (in press). DOI:10.1016/j.clinph.2010.04.018
4. Vanhatalo S, Palva JM, Holmes MD, et al. Infraslow oscillations modulate excitability and interictal epileptic activity in the human cortex during sleep. Proc Natl Acad Sci USA 2004;101:5053–5057.
5. Ikeda A, Terada K, Mikuni N, et al. Subdural recording of ictal DC shifts in neocortical seizures in humans. Epilepsia 1996;37:662–674.
6. Caspers H. Handbook of electroencephalography and clinical neurophysiology. Vol 10.Amsterdam: Elsevier, 1974:7–11.
7. Tallgren P, Vanhatalo S, Kaila K, Voipio J. Evaluation of commercially available electrodes and gels for recording of slow EEG potentials. Clin Neurophysiol 2005;116:799–806.
8. Dietzel I, Heinemann U, Lux HD. Relations between slow extracellular potential changes, glial potassium buffering, and electrolyte and cellular volume changes during neuronal hyperactivity in cat brain. Glia 1989;2:25–44.
9. Johnston D, Brown TH. Giant synaptic potential hypothesis for epileptiform activity. Science 1981;211:294–297.
10. Scemes E, Giaume C. Astrocyte calcium waves: what they are and what they do. Glia 2006;54:716–725.
11. Wolf F, Kirchhoff F. Neuroscience: imaging astrocyte activity. Science 2008;320:1597–1599.
12. Fields RD. Stevens-Graham B. New insights into neuron-glia communication. Science 2002;298:556–562.
13. Allen NJ, Barres BA. Neuroscience: glia-more than just brain glue. Nature 2009;457:675–677.
14. Angulo MC, Kozlov AS, Charpak S, Audinat E. Glutamate released from glial cells synchronizes neuronal activity in the hippocampus. J Neurosci 2004;24:6920–6927.
15. Fellin T, Pascual O, Gobbo S, et al. Neuronal synchrony mediated by astrocytic glutamate through activation of extrasynaptic NMDA receptors. Neuron 2004;43:729–743.
16. Tian GF, Azmi H, Takano T, et al. An astrocytic basis of epilepsy. Nat Med 2005;11:973–981.
17. Rosenow F, Lüders HO. Presurgical evaluation of epilepsy. Brain 2001;124:1683–1700.

18. Theodore WH, Fisher RS. Brain stimulation for epilepsy. Lancet Neurol 2004;3:111–118.

19. Le Van Quyen M, Martinerie J, Navarro V et al. Anticipation of epileptic seizures from standard EEG recordings. Lancet 2001;357: 183–188.

20. Mormann F, Andrzejak RG, Elger CE, Lehnertz K. Seizure prediction: the long and winding road. Brain 2007;130:314–333.

Large Genomic Deletions: A Novel Cause of Ullrich Congenital Muscular Dystrophy

A. Reghan Foley, MD,[1,2] Ying Hu, MS,[1] Yaqun Zou, MD,[1] Michele Yang, MD,[1,3] Līvija Medne, MS, CGC,[1,4] Meganne Leach, MSN, CRNP,[1] Laura K. Conlin, PhD,[4] Nancy Spinner, PhD,[5,6] Tamim H. Shaikh, PhD,[6,3] Marni Falk, MD,[4,6] Ann M. Neumeyer, MD,[7] Laurie Bliss,[7] Brian S. Tseng, MD, PhD,[7] Thomas L. Winder, PhD, FACMG,[8] and Carsten G. Bönnemann, MD[1,6,9]

Two mutational mechanisms are known to underlie Ullrich congenital muscular dystrophy (UCMD): heterozygous dominant negatively-acting mutations and recessively-acting loss-of-function mutations. We describe large genomic deletions on chromosome 21q22.3 as a novel type of mutation underlying recessively inherited UCMD in 2 families. Clinically unaffected parents carrying large genomic deletions of *COL6A1* and *COL6A2* also provide conclusive evidence that haploinsufficiency for *COL6A1* and *COL6A2* is not a disease mechanism for Bethlem myopathy. Our findings have important implications for the genetic evaluation of patients with collagen VI–related myopathies as well as for potential therapeutic interventions for this patient population.

ANN NEUROL 2011;69:206–211

Ullrich congenital muscular dystrophy (UCMD; MIM 254090), Bethlem myopathy (BM; MIM 158810) and phenotypes intermediate to UCMD and BM form a group of congenital muscular dystrophies known as the collagen VI–related myopathies.[1] Underlying these conditions is a decrease, absence, or dysfunction of the extracellular matrix protein collagen VI. The collagen VI heterotrimeric monomer is composed of 3 alpha chains: α1(VI), α2(VI), and α3(VI),[2,3] each containing a short triple helical domain flanked by globular domains. Assembly of collagen VI proceeds intracellularly with monomers aligning in an antiparallel fashion to form dimers, which then align laterally to form tetramers. The tetramers are secreted and align extracellularly in an end-to-end fashion, forming beaded microfilaments as the final product of collagen VI assembly.[4–6]

Mutations in any of the 3 genes coding for the 3 collagen VI alpha chains, *COL6A1*, *COL6A2*, or *COL6A3*, can affect the complex assembly and secretion of collagen VI, resulting in the phenotype of a collagen VI–related myopathy. *COL6A1* and *COL6A2* are located on chromosome 21q22.3 (Heiskanen and colleagues[7]) and *COL6A3* is located on chromosome 2q37 (Weil and colleagues[8]). UCMD results from either recessive or dominantly-acting mutations[9,10] and is characterized by a combination of early-onset muscle weakness, congenital contractures of the proximal joints, and hyperlaxity of the distal joints.[11] BM typically follows autosomal dominant inheritance; however, autosomal recessive inheritance has recently been described as well.[12,13] BM is characterized by slowly progressive muscle weakness and joint contractures.[14]

Here we describe a novel type of mutation underlying recessively inherited UCMD by delineating large genomic deletions on chromosome 21q22.3, resulting in loss of *COL6A2* or both *COL6A1* and *COL6A2*, and occurring in combination with a mutation in *COL6A2* or a deletion of *COL6A2* on the other allele to cause disease. We also conclusively demonstrate that haploinsufficiency for *COL6A1* and *COL6A2* is associated with decreased collagen VI deposition but is not associated with clinical neuromuscular disease.

Patients and Methods

Clinical details were collected according to a protocol approved by the institutional review board and are summarized in the Table 1.

From the [1]Division of Neurology, [4]Division of Human Genetics, [5]Division of Pathology, The Children's Hospital of Philadelphia, University of Pennsylvania, Philadelphia, PA; [2]Dubowitz Neuromuscular Centre, University College London Institute of Child Health and Great Ormond Street Hospital for Children, London, UK; [3]Department of Pediatrics, University of Colorado Denver, Aurora, CO; [6]Department of Pediatrics, University of Pennsylvania, Philadelphia, PA; [7]Department of Neurology, Massachusetts General Hospital, Harvard University, Boston, MA; [8]Prevention Genetics, Marshfield, WI; [9]Neuromuscular and Neurogenetic Disorders of Childhood Section, Neurogenetics Branch, National Institute of Neurological Disorders and Stroke/NIH, Bethesda, MD.

Address correspondence to Dr Bönnemann, Neuromuscular and Neurogenetic Disorders of Childhood Section, Neurogenetics Branch, National Institute of Neurological Disorders and Stroke/NIH, Porter Neuroscience Research Center, Building 35, Room 2A-116, MSC 35 Convent Drive, Bethesda, MD 20892-3705. E-mail: carsten.bonnemann@nih.gov

Received Jun 23, 2010, and in revised form Sep 9, 2010. Accepted for publication Sep 24, 2010.

View this article online at wileyonlinelibrary.com. DOI: 10.1002/ana.22283

Uneven Interhemispheric Connections Between Left and Right Primary Sensori-Motor Areas

Kiyohito Terada,[1]* Shuichi Umeoka,[2] Naotaka Usui,[2] Koichi Baba,[2] Keiko Usui,[1] Shigeru Fujitani,[2] Kazumi Matsuda,[2] Takayasu Tottori,[2] Fumihiro Nakamura,[3] and Yushi Inoue[3]

[1]*Department of Neurology, National Epilepsy Center, Shizuoka Institute of Epilepsy and Neurological Disorders, Aoi-ku, Shizuoka 420-8688, Japan*
[2]*Department of Neurosurgery National Epilepsy Center, Shizuoka Institute of Epilepsy and Neurological Disorders, Aoi-ku, Shizuoka 420-8688, Japan*
[3]*Department of Psychiatry, National Epilepsy Center, Shizuoka Institute of Epilepsy and Neurological Disorders, Aoi-ku, Shizuoka 420-8688, Japan*

Abstract: To clarify the characteristics of interhemispheric connections, we investigated cortico-cortical evoked potentials (CCEP) in human. Fourteen patients with temporal lobe epilepsy who underwent invasive EEG monitoring with bilaterally implanted subdural electrodes were studied. Electric pulse stimuli were given in a bipolar fashion at two adjacent electrodes on and around the motor area (MA) or sensory area (SA), and CCEP responses were recorded by averaging electrocorticograms from the contralateral hemisphere. Seventy-two pairs of electrodes were stimulated, and 468 recordings were analyzed. Fifty-one of 468 recordings demonstrated CCEP responses. Of 51 responses, 16 consisted of an initial positive triphasic wave (Type 1), 27 had an initial negative biphasic wave (Type 2), and 8 showed an initial positive biphasic wave (type 3). The mean latencies of the earliest peaks were 13.1, 28.9, and 29.4 ms in Types 1, 2, and 3 responses, respectively. The responses were more frequently evoked by stimulating facial MA (f-MA) and nonfacial MA (nf-MA) than by stimulating SA or noneloquent area. In both f-MA and nf-MA stimulation, the responses were more frequently recorded at the contralateral f-MA than at the contralateral nf-MA or other areas. SA stimulation never evoked CCEP responses at the contralateral MA or SA. The amplitudes were maximal when f-MA was stimulated and responses recorded at the contralateral f-MA. These findings suggest that the interhemispheric connections are uneven. Both f-MA and nf-MA send dense interhemispheric connections to the contralateral f-MA. SA may have no or only rare direct connection with the contralateral MA or SA. *Hum Brain Mapp 00:000–000, 2011.* © **2011 Wiley-Liss, Inc.**

Key words: neural networks; corpus callosum; human brain; primary motor cortex; primary sensory cortex; intracranial recording; subdural electrode; functional mapping; evoked potentials; epilepsy

INTRODUCTION

Neural connections in the human brain have attracted interest recently, and human neural pathways have been demonstrated by MRI studies [Mori et al., 2000]. Electrophysiologically, these connections may also be examined by cortico-cortical evoked potential (CCEP) studies [Brugge et al., 2003; Greenlee et al., 2004; Matsumoto et al., 2004, 2005, 2007; Rutecki et al., 1989; Terada et al., 2008; Umeoka et al., 2009; Wilson et al., 1990, 1991].

Previously, we recorded CCEP responses from the contralateral hemisphere by stimulating facial motor area

Contract grant sponsor: Ministry of Health, Labor and Welfare; Contract grant number: 19A-6; Contract grant sponsor: Japan Epilepsy Research Foundation.

*Correspondence to: Kiyohito Terada, Department of Neurology, National Epilepsy Center, Shizuoka Institute of Epilepsy and Neurological Disorders, 886 Urushiyama, Aoi-ku, Shizuoka 420-8688, Japan. E-mail: kyht-terada@umin.net

Received for publication 17 May 2009; Revised 28 June 2010; Accepted 19 September 2010

DOI: 10.1002/hbm.21189

Published online in Wiley InterScience (www.interscience.wiley.com).

TABLE I. Number of electrodes identifying eloquent areas by standard cortical stimulations, and number of electrodes recording CCEP responses for each area stimulated

		Standard cortical stimulation			Cortico-cortical evoked potential study															
					Stimulated area															
		Number of electrodes identifying eloquent areas			f-MA				nf-MA				SA				NEA			
					Number of electrodes recording CCEP in each area															
Pt.	Sex/ age	f-MA	nf-MA	SA	f-MA	nf-MA	SA	NEA	f-MA	nf-MA	SA	NEA	f-MA	nf-MA	SA	NEA	f-MA	nf-MA	SA	NEA
1	F/36			2											2	6				
2	F/32	2	2		1	1		4	1	1		4					8	8		44
3	M/29			2												4				8
4	M/36	3			4			8												
5	F/21	3			4			8									2			2
6	F/21	1		1				4								4	1		1	17
7	M/21	4	2		4	2		6	2	1		3					4	2		6
8	F/22																			5
9	F/43	6		2	8		4	18					8			12	14		6	30
10	M/35		2	3					2	3	5			2	3	5		1	2	1
11	F/34	4		2			4	12					4			4	8		8	32
12	F/29	1		4									2		4	8	2		8	20
13	F/16	4	2		6	4		8	2			4					4	2		6
14	M/23																			10

Pt, patient number; M, male; F, female; f-MA, facial motor area; nf-MA, nonfacial motor area; SA, somatosensory area; NEA, noneloquent area.

(f-MA) in three epilepsy patients [Terada et al., 2008]. Our result demonstrated that most of these interhemispheric CCEP responses showed initial positive triphasic waveforms (P1-N1-P2). P1 had 1 or 2 notches, although P1 was absent in two of eight responses. The latency of P1 ranged 9.2 to 23.8 ms. The response was not evoked when non-motor area (non-MA) was stimulated, while stimulation of the motor area (MA) evoked CCEP responses at both MA and non-MA electrodes in the contralateral hemisphere. Therefore, we speculate that the stimulation produces one-way volley, and that orthodromic impulses may play an important role for this CCEP response. Regarding the location relationship between stimulation and response, stimulation of upper areas evoked responses recorded from the upper areas, while stimulation of lower areas produced responses recorded from the lower areas. These findings suggest that the neural connections may project to contralateral homonymous areas. However, our previous study examined only a small number of patients and evaluated only the f-MA. Therefore, we were not able to characterize the interhemispheric connections between bilateral MA more precisely.

In this study, we evaluated 468 CCEP recordings from 14 epilepsy patients to clarify the characteristics of interhemispheric neural connections arising from the MA. Furthermore, we also succeeded to stimulate the sensory area (SA) and evaluated interhemispheric connections originating from the SA.

SUBJECTS AND METHODS

Subjects, Electrodes Implantation, and Functional Mapping

The data were obtained from 14 patients with medically intractable temporal lobe epilepsy (5 men and 9 women, aged 16–43 years) (Table I). The Institutional Review Board approved this study, and informed consent was obtained from all patients. Interictal neurological examinations detected no focal neurological abnormalities in all patients. Routine noninvasive evaluations including MRI, SPECT, and scalp EEG/video monitoring failed to determine the epileptogenic zone. Therefore, these patients underwent long-term invasive EEG/video monitoring with chronically implanted subdural and depth electrodes as a part of presurgical evaluation [Mihara and Baba, 2001].

Each subdural electrode was 2.3 mm in diameter and made of platinum-iridium alloy. The center-to-center interelectrode distance was 10 mm. The locations and the numbers of subdural and depth electrodes implanted were standardized (see Fig. 1) [Mihara and Baba, 2001]. Briefly, two bundles of depth electrodes were inserted targeting

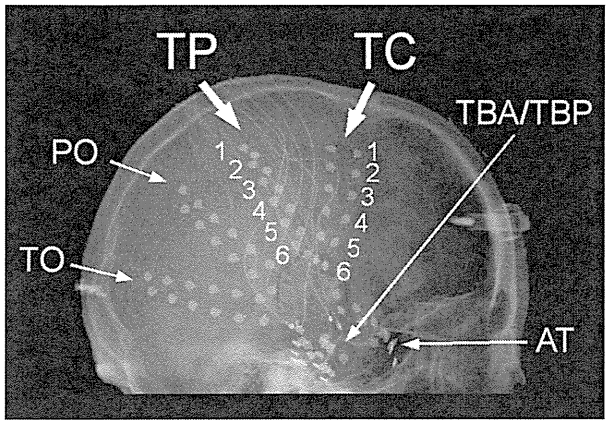

Figure 1.
X-ray image showing the standardized locations of subdural electrodes. Subdural plates (2 × 6; TBA and TBP) cover basal temporal regions, and 5 subdural strips (1 × 6) cover extratemporal areas on each side (AT, anterior temporal; TC, temporo-central; TP, temporo-parietal; PO, parieto-occipital; and TO, temporo-occipital). Plates and strips were placed almost symmetrically on both sides. The tip electrode of each bundle was designated "1," and the number is increased in order up to "6" for the most proximal electrode.

the amygdala and hippocampus on each side. A subdural plate (2 × 6) was slipped under the basal temporal lobe on each side. To detect epileptiform activities of extra-temporal areas, a subdural strip (1 × 6) was placed to cover the anterior temporal region (AT), and four strips were slipped radially from the burr hole to cover the temporo-central (TC), temporo-parietal (TP), parieto-occipital (PO), and temporo-occipital regions (TO). All bundles, plates, and strips were placed almost symmetrically on both sides. The tip electrode of each bundle was designated "1," and the number was increased in order up to "6" for the most proximal electrodes.

Standard cortical stimulation was performed [Lesser and Gordon, 2000] to determine the MA, SA, and other eloquent areas. A constant-current biphasic square electric pulse with a duration of 0.3 ms and frequency of 50 Hz was delivered for 1 to 5 sec (SEN-3301/SSI04J, Nihon Koden Corp., Tokyo). When pure motor or sensory response was evoked upon stimulation of an electrode, the electrode was defined as MA or SA. If both motor and sensory responses were observed at a single electrode, such electrode was excluded from further CCEP analysis in this study. The f-MA (MA of mouth, tongue, or face) and nonfacial MA (nf-MA; MA of finger or hand) were analyzed separately because CCEP responses of these areas have different characteristics.

The locations of electrodes were also anatomically confirmed by using 3D reconstruction MRI imaging (MRI-Cro: "http://www.cabiatl.com/mricro/") in each patient. Electrodes locating on the precentral gyrus were defined as MA-MRI, and electrodes on the postcentral gyrus were defined as SA-MRI. When electrodes were not on the precentral or postcentral gyri, they were named NEA-MRI.

Stimulation and Data Acquisition for CCEP

CCEP recordings were performed after clinical evaluations were completed, and therefore did not interfere with clinical evaluations. All CCEP recordings were performed while the patients were awake and sitting in bed.

For CCEP recording, we conducted stimulation by applying the same parameters as in the previous reports [Terada et al., 2008; Umeoka et al., 2009]. Briefly, the electrical stimulation consisted of a constant-current square pulse at a duration of 0.3 ms with a frequency of 1 Hz in alternating polarity (SEN-3301/SSI04J, Nihon Koden Corp., Tokyo). Two adjacent electrodes were stimulated in bipolar fashion. As we analyzed f-MA, nf-MA, and SA stimulations separately, we did not use the responses evoked by simultaneous stimulation of different eloquent areas; e.g., stimulation of an electrode pair covering f-MA and nf-MA. For the same reason, we did not use the responses evoked by stimulation of an electrode pair covering MA-MRI and SA-MRI. For comparison, not only eloquent areas, but also noneloquent areas (NEA) were stimulated for CCEP recording. The current intensity was set at 80% of the intensity that produced clinical signs or after-discharges during standard cortical stimulation for eloquent areas. For NEA, 80% of the maximal intensity employed in cortical stimulation was used. Even using lower stimulus intensity, patients sometimes demonstrated clinical responses during CCEP recording. In such cases, we decreased the intensity until no clinical response was observed. No clinical seizure occurred during CCEP recordings.

For CCEP recording, an evoked potential machine was used (Neuropack sigma, Nihon Koden Corp., Tokyo). Sampling rate was set at 5,000–10,000 Hz. The low frequency filter was set at 10 Hz, and the high frequency filter at 2,000–5,000 Hz depending on the sampling rate. Electrocorticograms were recorded with reference to a subdural electrode placed on a noneloquent indifferent area. For CCEP recording, 20 to 50 electrocorticographic responses were averaged and time-locked to the stimulus.

For statistical analyses, chi-square test and *t*-test were used (StatMate III, Advanced Technology for Medicine & Science, Tokyo).

RESULTS

Cortical stimulation identified the f-MA (28 electrodes), nf-MA (8 electrodes), and SA (16 electrodes including 8 electrodes for facial SA and 8 electrodes for nonfacial SA) in 14 patients (Table I). All these eloquent areas were detected by stimulating electrodes of the TC or TP strips (see Fig. 1). Therefore, CCEP were evaluated by

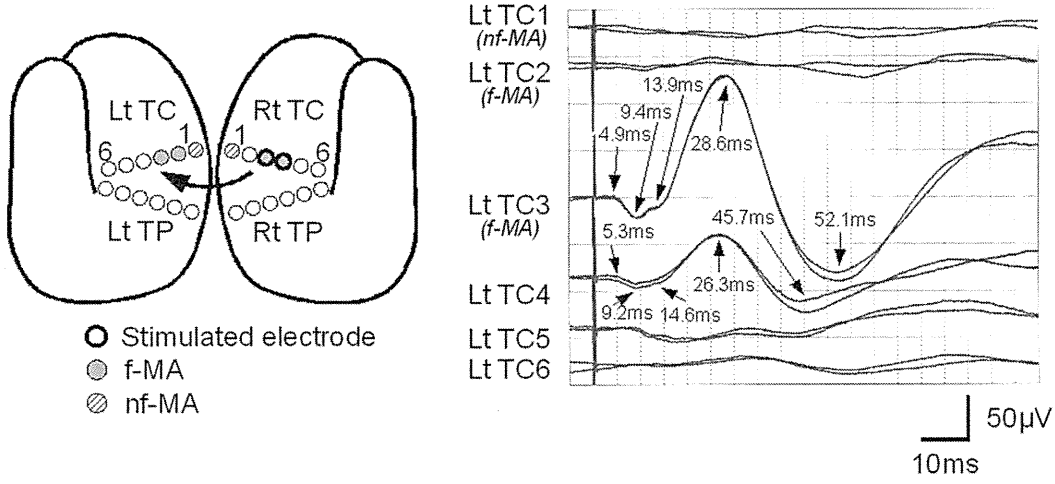

Figure 2.

Typical Type I response observed in Patient 7. The schematic figure shows the location of eloquent area and the stimulated electrodes. Bold circles signify the stimulated electrodes. Gray circles indicate electrodes located over facial motor area (f-MA), and hatched circles over nonfacial motor area (nf-MA). Two waveforms are displayed in each channel to confirm their reproducibility. CCEP responses were evoked by stimulating f-MA (Rt TC3/4), and were recorded from contralateral electrodes. The third and fourth channels (Lt TC3 on f-MA and Lt TC4 on non-eloquent area) demonstrate initial positive triphasic waveforms. Although there may be responses at the fifth and sixth channels, they are not analyzed in this study because they are too small.

stimulating TC or TP electrodes and recording from the contralateral TC or TP electrodes. As transcallosal CCEP responses were well recognized at the contralateral homologous area in the previous study [Terada et al., 2008], the homonymous electrodes and their contiguous electrodes were mainly selected as recording sites. Because of time pressure, not all pairs could be examined. Finally, we stimulated a total of 72 pairs of electrodes, and 468 recordings were evaluated (Table I). Of 468 recordings, 51 demonstrated definitive CCEP responses and were used in subsequent analyses.

Waveforms

As reported previously, initial positive triphasic waves (P1-N1-P2) were recorded from the contralateral hemisphere (Figs. 2–4; Type 1 response). Type 1 responses were found in 16 recordings; 12 by f-MA stimulation, 2 by SA stimulation, and 2 by NEA stimulation. The recorded sites were the f-MA (seven responses), SA (one response), and NEA (eight responses). The mean onset latency was 5.2 ms [standard deviation (SD): 1.0], and the mean latencies of P1, N1, and P2 were 13.1 ms (SD: 3.3), 30.1 ms (SD: 2.9), and 56.9 ms (SD: 7.9), respectively. The mean amplitude was 16.0 μV (SD: 8.7) from onset to P1, 77.3 μV (SD: 59.4) from P1 to N1, and 107.9 μV (SD: 72.2) from N1 to P2. A notch was seen superimposing on P1 in all Type 1 responses except one, in which 2 notches were detected (see Fig. 3).

In 27 recordings, initial negative biphasic waves (N1-P2) were observed (Fig. 5; Type 2 response). Type 2 responses were obtained by f-MA stimulation (16 responses), nf-MA stimulation (6 responses), and NEA stimulation (5 responses). The recorded sites were the f-MA (9 responses), nf-MA (1 response), SA (1 response), and NEA (16 responses). The mean onset latency was 11.1 ms (SD: 3.7), and latencies of N1 and P1 were 28.9 ms (SD: 5.0) and 52.5 ms (SD: 8.9), respectively. The mean amplitude was 27.5 μV (SD: 17.2) from onset to N1, and 49.1 μV (SD: 27.4) from N1 to P2. In 7 of 27 responses, a notch was seen superimposing on N1 (see Fig. 5). This notch was observed when stimulating f-MA (4 responses), nf-MA (1 response), or NEA (2 responses), and recorded at f-MA (3 responses) or NEA (4 responses).

In addition, initial positive biphasic waveforms (P1′-N1′) were identified in 8 recordings (Fig. 6; Type 3 response). Type 3 responses were obtained by f-MA stimulation (four responses), nf-MA stimulation (one responses), or NEA stimulation (three responses), and recorded at f-MA (five responses), nf-MA (two responses), or NEA (one response). The mean latencies of onset, P1′ and N1′ were 17.0 ms (SD: 6.0), 29.4 ms (SD: 4.5), and 49.4 ms (SD: 5.7), respectively. The mean amplitude was 20.9 μV (SD: 10.9) from onset to P1′, and 34.6 μV (SD: 16.5) from P1′ to N1′.

Statistical Analysis

Comparison among stimulation and recording sites

Chi-square test was used to analyze the effect of the stimulation site. The analysis demonstrated that the

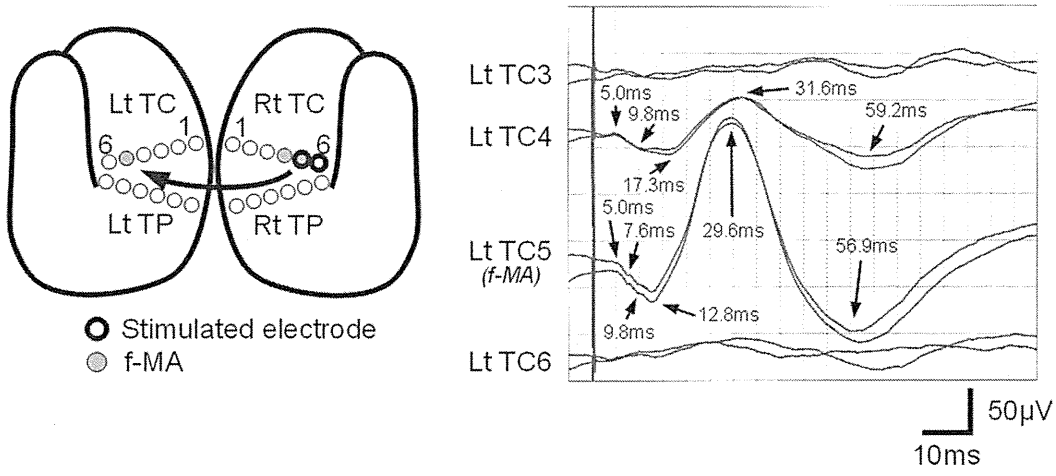

Figure 3.

Type I response observed in Patient 5. The schematic figure shows the location of eloquent area and the stimulated electrodes. Bold circles signify the stimulated electrodes. Gray circles indicate electrodes located over facial motor area (f-MA). Two waveforms are displayed in each channel to confirm their reproducibility. CCEP responses were evoked by stimulating an electrodes pair including f-MA (Rt TC5), and were recorded from contralateral electrodes. The second and third channels (Lt TC4 on noneloquent area and Lt TC5 on f-MA) demonstrate initial positive triphasic waveforms.

stimulating site affected the positive CCEP response rate ($P < 0.001$). In each comparison between eloquent sites, a significant difference was observed between f-MA and SA ($P < 0.001$), between f-MA and NEA ($P < 0.001$), between nf-MA and SA ($P < 0.001$), and between nf-MA and NEA ($P < 0.001$) (Table II). These findings thus suggested that f-MA stimulation and nf-MA stimulation evoked contralateral hemispheric CCEP responses more frequently than SA stimulation or NEA stimulation.

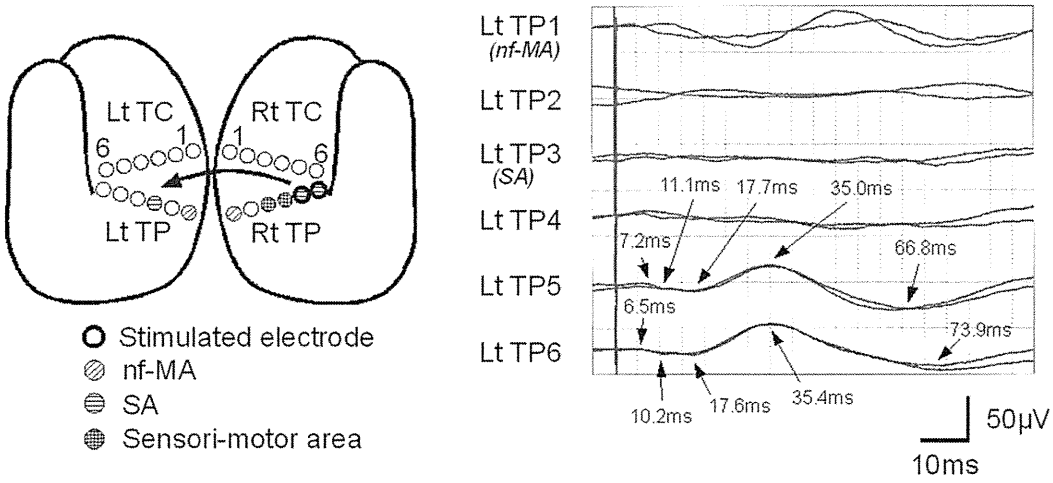

Figure 4.

Type I response observed in Patient 10. The schematic figure shows the location of eloquent area and the stimulated electrodes. In addition to the symbols described in Figure 2, sensory area (SA; circle with horizontal lines) and sensori-motor area (circle with crossed lines) are demonstrated. CCEP responses were evoked by stimulating SA (Rt TP5/6), and were recorded from contralateral electrodes. The fifth and sixth channels (Lt TP5/6 on noneloquent area) demonstrate initial positive triphasic waveforms. Although the first channel may show some response, it is not used in subsequent analysis because it is not reproducible.

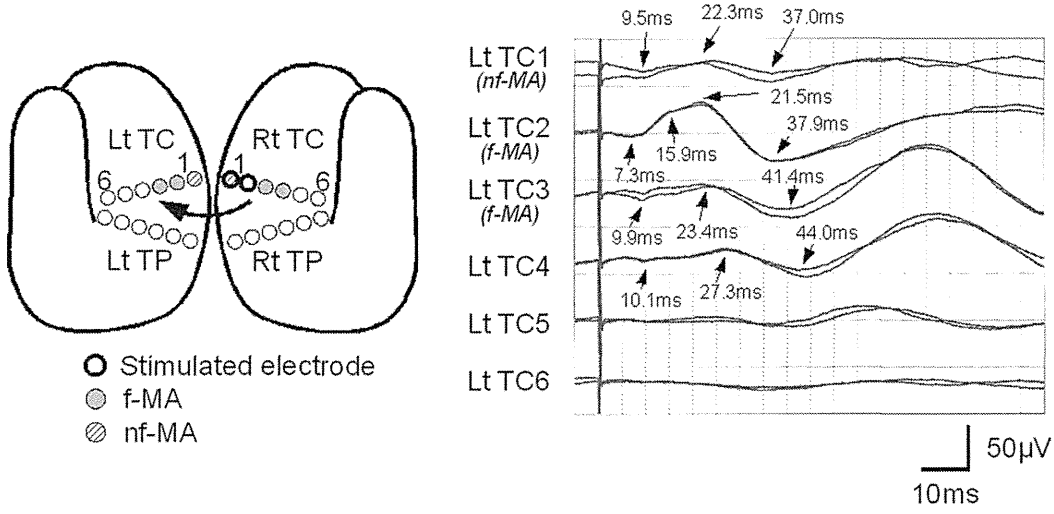

Figure 5.

Typical Type 2 responses observed in Patient 7. The schematic figure shows the location of eloquent area and the stimulated electrodes (see Fig. 2 for explanation). CCEP responses are evoked by stimulating nonfacial motor area (nf-MA; Rt TC1) and noneloquent area (NEA; Rt TC2), and were recorded from contralateral electrodes. The first, second, third, and fourth channels (Lt TC1 on nf-MA, Lt TC2/3 on facial motor area [f-MA] and Lt TC4 on NEA) demonstrate initial negative biphasic waveforms. At Lt TC2, the initial negative peak (N1) has a notch at 15.9 ms.

Chi-square analysis on the effect of the recording site demonstrated that the recording site was important for a positive contralateral CCEP response for f-MA and nf-MA stimulations ($P < 0.01$ and $P < 0.05$, respectively), but had no significant effect for SA and NEA stimulations (Table II). For f-MA stimulation, a significant difference in positive CCEP response was found between f-MA and SA recordings ($P < 0.05$) and between f-MA and NEA recordings ($P < 0.005$). For nf-MA stimulation, a significant difference was also observed between f-MA and SA recordings

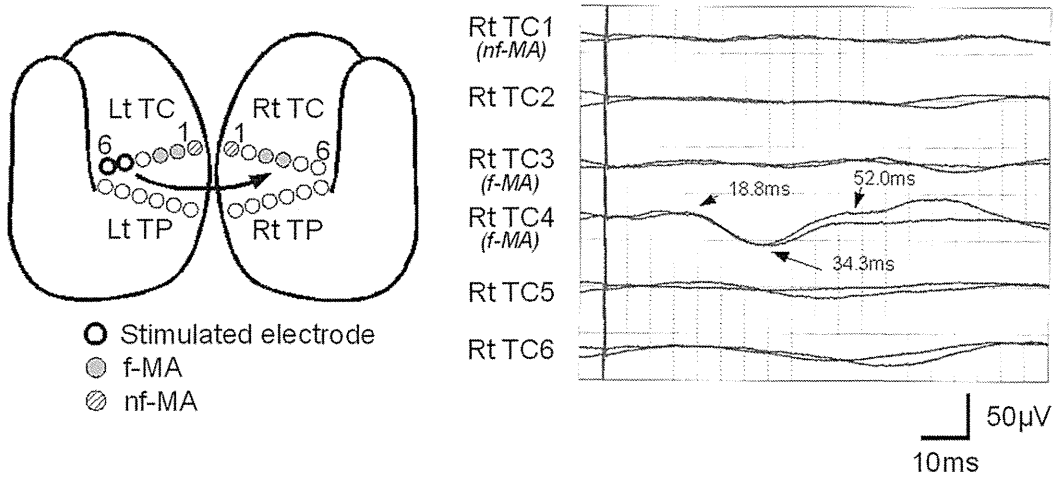

Figure 6.

Typical Type 3 responses observed in Patient 7. The schematic figure shows the location of eloquent area and the stimulated electrodes (see Fig. 2 for explanation). CCEP responses are evoked by stimulating noneloquent area (NEA; Lt TC5/6), and were recorded from contralateral electrodes. The fourth channel (Rt TC4 on facial motor area [f-MA]) demonstrates an initial positive biphasic waveform.

TABLE II. Number of trials and responses recorded from stimulation of pairs of electrodes (for cortical stimulation-defined eloquent areas)

Stimulation	Recording	Number of trials	CCEP response		Mean response rate per stimulation area	Response type		
			Number	%		Type 1	Type 2	Type 3
f-MA	f-MA	27	15	55.6[a]	29.1[b]	7	5	3
	nf-MA	7	1	14.3				1
	SA	8	1	12.5			1	
	NEA	68	15	22.1		5	10	
nf-MA	f-MA	5	4	80.0[a]	25.0[b]		3	1
	nf-MA	4	1	25.0			1	
	SA	3	0	0				
	NEA	16	2	12.5			2	
SA	f-MA	14	0	0	2.9			
	nf-MA	2	0	0				
	SA	9	0	0				
	NEA	43	2	4.7		2		
NEA	f-MA	43	2	4.7	3.8		1	1
	nf-MA	13	1	7.7				1
	SA	25	1	4.0		1		
	NEA	181	6	3.3		1	4	1

f-MA, facial motor area; nf-MA, nonfacial motor area; SA, somatosensory area; NEA, noneloquent area.
[a]Significantly higher rate compared with SA ($P < 0.05$), and NEA recording ($P < 0.005$).
[b]Significantly higher rate compared with SA stimulation ($P < 0.001$) and NEA stimulation ($P < 0.001$).

($P < 0.05$) and between f-MA and NEA recordings ($P < 0.005$). These data suggested that both f-MA and nf-MA stimulations tended to evoke contralateral CCEP responses at the f-MA.

The same statistical analysis was performed among MA-MRI, SA-MRI, and NEA-MRI (Table III). The statistical analysis demonstrated that the stimulating site affected the positive CCEP response rate ($P < 0.001$). In each comparison between eloquent sites, a significant difference was observed between MA-MRI and SA-MRI ($P < 0.001$), between MA-MRI and NEA-MRI ($P < 0.001$), and between SA-MRI and NEA-MRI ($P < 0.01$) (Table III). These findings indicated that both MA-MRI stimulation and SA-MRI stimulation evoked contralateral hemispheric CCEP responses more frequently than NEA-MRI stimulation, and that MA-MRI stimulation evoked the responses much more frequently than SA-MRI stimulation.

TABLE III. Number of trials and responses recorded from stimulation of pairs of electrodes (for MRI-defined eloquent areas)

Stimulation	Recording	Number of trials	CCEP response		Mean response rate per stimulation area	Response type		
			Number	%		Type 1	Type 2	Type 3
MA-MRI	MA-MRI	53	19	35.8[a]	25.4[b]	5	10	4
	SA-MRI	29	8	27.6		3	5	
	NEA-MRI	56	8	14.3		4	4	
SA-MRI	MA-MRI	45	7	15.6	8.8[c]	3	2	2
	SA-MRI	38	3	7.9		1	2	
	NEA-MRI	64	3	4.7			2	1
NEA-MRI	MA-MRI	47	1	2.1	1.8			1
	SA-MRI	34	1	2.9			1	
	NEA-MRI	83	1	1.2			1	

MA-MRI, motor area defined by MRI imaging; SA-MRI, somatosensory area defined by MRI imaging; NEA-MRI, noneloquent area defined by MRI imaging.
[a]Significantly higher rate compared with NEA-MRI recording ($P < 0.01$).
[b]Significantly higher rate compared with SA-MRI stimulation ($P < 0.001$) and NEA-MRI stimulation ($P < 0.001$).
[c]Significantly higher rate compared with NEA-MRI stimulation ($P < 0.01$).